Chapter

Photovoltaic Parameters Affecting the Efficiency and Stability of Perovskite Photovoltaic Devices

Asha Chauhan, Anjali Oudhia and Ashok Kumar Shrivastav

Abstract

Perovskite photovoltaic devices (PVDs) have emerged as excellent futuristic photovoltaic energy-harvesting material in the past few years with a remarkable efficiency of over 25%. The intense scientific research in the field of perovskite photovoltaic technologies further enables their goal of effective commercialization. The device's efficiency strongly relies on the optical, morphological and electrical properties of the emerged charge collective and perovskite layer. This chapter critically articulates the advancements made by the choice of charge collecting layer to get the optimum PVDs. Further, the challenges of lead toxicity and the possible replacement with green non-toxic perovskite will also be discussed. The influence of photovoltaic parameters such as the thickness, bandgap, electron affinity, mobility, dielectric permittivity, density of states, donor and acceptor density and defect level on the device's performance and stability are introduced in this chapter. The chapter also analyzes the impact of series resistance caused by various factors such as bulk resistance, circuit connection and contacts, uneven morphology, defects and voids/vacancies and trap states at grain boundaries of the perovskite layer. This chapter focuses on elucidating the theoretical mechanisms to optimize the photovoltaic performance of the device by tuning the photovoltaic properties and material modeling of different stoichiometry.

Keywords: photovoltaic device, perovskite, photovoltaic parameters, optimization, energy and efficiency

1. Introduction

1.1 Worldwide energy demand

Energy is essential to life and key to industrial development for the advancement of the economic and social well-being of the world population. The daily growth of the world population accelerated energy usage and consumption, resulting in an energy crisis and environmental pollution. The earth takes millions of years to fertilize and

store the fuels. In the long history of human existence, the consumption of fossil fuels is a pulse action of relatively short duration owing to their exhausting supply and environmental impact. Fossil fuels (oil, coal, and natural gas) have major impacts on the environment and living things because their use is the emission of greenhouse gases, which leads to global warming and climate change. The new era of technology and industrialization is increasing the consumption and demand of energy all over the world. Hence, the requirement for alternate-sustainable and eco-friendly energy resources has risen, which can fulfill the energy hunger of the growing human population and replace fossil fuel sources. Due to the rising worldwide energy demand, new terms like the efficiency of energy, vulnerability in the supply, and the effects on the environment are becoming very popular.

The global energy consumption is estimated to be 580 million terajoules due to rapid economic expansion, population, urbanization, and industrialization. Environmental Impact Assessment (EIA) expects that the global energy demand to be increased by 47% in the next 30 years driven by recent technology vogues like machine learning, big data analytics, communication infrastructure like 5G, and the standard of living, centralized and standardized digital models. Petroleum Planning and Analysis Cell (PPAC), a unit of the federal oil ministry, released a report stating that the fuel demand in India could rise to 214.5 million tons in the next 30 years. The demand for gasoline, diesel, aviation fuel, petcoke (a better-burning alternative to coal), liquefied petroleum gas, and cooking fuel is estimated to grow by 10%. The huge energy demand in the various sector from households to industry could be met only by harnessing all available resources of energy. Also, to avail the natural energy resources for a longer period and for next-generation mankind, their conservation without affecting the productivity and targets is a must duty of the inhabitations of this planet. It is a must to develop energy conservation techniques, methods, and energy-saving projects and training. These methods are as simple as installing more insulation in the house, getting used to public transportation, and energy audit services like diesel use analysis, green workplace lightening, heat loss, efficiency, and planning for improvement in production. The oversized, overloaded, and overheated machines eat the energy and compress the machine's efficiency. The audit of energy usage, housekeeping, and maintenance of machines can reduce the consumption of energy by up to 5%.

The worldwide rapid consumption of fossil fuel resources is a subject of concern and urgently requires an alternate, trustworthy, and non-fossil fuel resource of energy to meet the energy demands for the immediate future and the upcoming generation. Renewable or sustainable non-fossil fuels such as the sun, wind, and water are derived from naturally replenished sources or processes of the earth. The most common sustainable energy resources are as follows: wind energy, solar energy, hydroelectric energy, geothermal energy, bioenergy, nuclear energy, hydrogen energy, tidal energy, and wave energy. Out of these energy resources, nuclear and solar energy stand out as the brightest long-range and traditional sources of energy that can fulfill the continuous energy demand. Nuclear energy originated from the process of putting light atoms together is called the nuclear fusion process. The earth has an abundant source of nuclear materials which makes it an alternative resource. Unfortunately, the radioactive waste from nuclear power plants and reactions has a great impact on the environment and climate. Constructing, monitoring, and maintaining nuclear power plants requires well-trained and skilled laborers. The need for huge investment and advanced technology are other drawbacks of nuclear power plants. Also, a nuclear accident can cause major damage to the health issues of living beings and the

DOI: http://dx.doi.org/10.5772/intechopen.115213

environment. From there, nuclear energy cannot be reasonably expected as the ultimate energy solution shortly.

The issues of nuclear pollution could be resolved by inexhaustible and renewable solar energy. Solar power is expanding exponentially throughout the world since it is a form of pollution-free light radiation and heat. A range of cost-effective technology to harness solar energy has been developed, such as solar photovoltaic, solar heating, and solar thermal electricity. Solar energy is used in water heating, heating buildings, power generation, photovoltaic conversion, solar cookers and ovens, solar drying of agricultural products, solar wind energy, etc. Modern solar technologies diversify the energy source and save money by large-scale electricity generation from solar energy.

1.2 Worldwide solar energy availability

Solar energy is an abundant energy source on Earth. Solar energy is a freely available and environmentally clean source of light like fossil fuels and nuclear energy. Solar radiation originates from nuclear fusion reactions that occur inside the core of the sun and the reaction produces the energy that keeps the sun hot. Sun is a massive nuclear reactor and 4 million of hydrogen is being converted into helium. In nuclear fusion, 4 hydrogens are converted into one helium, and some fraction of mass is released in the form of energy. The produced energy from the core of the sun is transmitted to the earth through electromagnetic radiation in the form of energy packets or quanta (photons). Sun strikes the earth continuously with a total of 173,000 terawatts of solar energy at a rate of 5E+24 Joule per year, which is more than 1000 times the energy produced by the world. Out of this huge number, only 6000 TWh of energy is converted into various forms of renewable energy (**Figure 1**) [1].

The energy produced per hour could meet the requirement of world energy for 1 year. However, due to atmospheric attenuation, not all part of the sunlight reaches the earth's surface. About 30% of sunlight is reflected in space and only 70% is absorbed

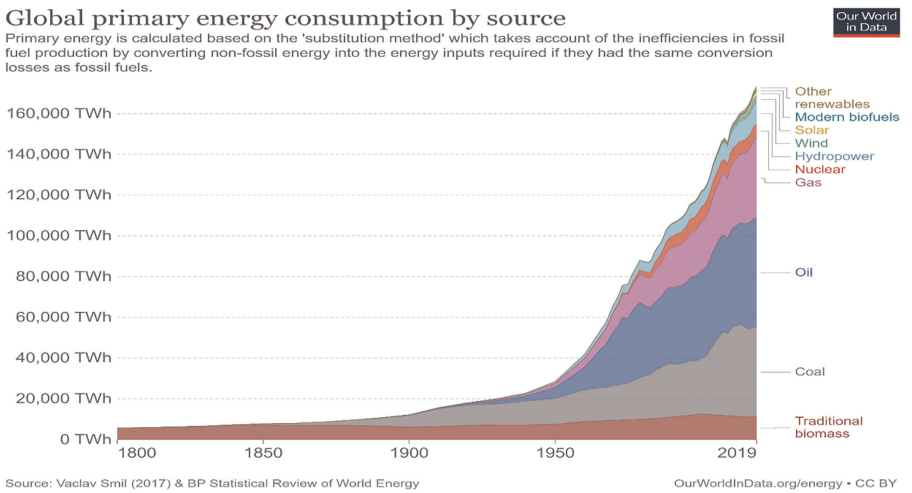


Figure 1.
Global direct primary energy consumption from 1800 until 2019. (Source: https://ourworldindata.org/grapher/global-primaryenergy?country=~OWID_WRL) [1].

on the earth's surface. About 16 out of 70% of absorbed light on the earth's surface is absorbed by dust and water vapor. The other 3% is absorbed by the clouds. Currently, solar energy is not being used as the primary resource of fuel energy; however, intense research work is required to harvest and store more energy from the sun to meet the high-energy demand of the world.

To harness solar energy, various sophisticated and modern photovoltaic (PV) technologies have been developed. Upon exposure to sunlight, the material produces electrical energy known as the photovoltaic effect. A solar cell is a photovoltaic device that converts light energy into electrical energy. An assembly of individual PV cells mounted in a framework for the installation is called solar panels. A collection of solar panels is called a PV panel and a sequence of PV panels is termed an array. The array of PV systems supplies electricity to the electrical device and equipment. The PV panels usually convert 15–22% of solar energy into electrical energy. The installation of solar panels can make a significant difference to the planet. The world implanted 260 GW of solar power plants and it is expected that in the future, this number will increase dramatically. In the United States, 1 GW of solar power is utilized for residential purposes. According to the report of the International Energy Agency (IEA), the process of converting photon energy into light energy is 720 TWh and it is expected to grow up to 1940 TWh in the upcoming years.

Despite harnessing solar energy, some common issues are associated with its use. The solar cells have intermittency issues and solar energy is diluted. According to Stefan-Boltzmann, the available solar radiation flux at the sun's surface is 63E+6 W/m^2. But in the hottest place on the earth, its availability is 1373 W/m^2, which is significantly low for PV devices and technological utilization of solar energy. It means that during night time and cloudy or rainy weather, solar radiation is not continuously available to generate electrical energy. Also, the availability of solar energy varies widely at different locations and under various weather conditions. Consequently, a large area of production and storage of electrical energy is required for many opto-electronic and PV device applications and it increases the total operating cost of the device. Thus, the main challenge for solar energy in the twenty-first century is its storage. So, the stored energy can be used in the event of a power outage. The researcher needs to develop a cost-effective and pollution-free method to collect and store the energy obtained from solar energy. This will prolong its utilization and help maintain a balance between the generation of electricity and the energy demand.

Another major challenge of solar energy is to improve the light absorbance property of solar cell materials. To harvest more energy from the sun needs to be absorbed more photons by the light-harvesting material. So, the light-harvesting material of the solar device can produce a huge number of excitons to get unprecedented performance from the device. Thus, we are required to find new excellent quality materials to use in the solar device. Among these factors, it is also worth noting that solar panels are implemented in the outer atmosphere and the decomposition of the solar cells in the ambient environment (oxygen and moisture) is also a big problem. The sensitivity toward moisture deteriorates and limits the actual performance of the solar device. The degradation mechanism and decomposition of the device need to be explored at ground level and need to look for strategies suppressing the thermal stability. Thus, it is required to deal with a lot of challenges of the solar cell to consider solar energy as an alternative energy resource. Intense, innovative, and seminal scientific works are required to modify the worldwide energy picture in the upcoming future which will help in power generation, creating a cleaner world, and improving our daily lives. Solar energy can be utilized in many different ways as the sun creates two types of

DOI: http://dx.doi.org/10.5772/intechopen.115213

energy: (i) light and (ii) heat. These forms of solar energy can be harnessed by both nature and human beings from photosynthesis in plants to PV cells, solar power, heating water and food, heating buildings, solar lighting, and solar wind energy.

1.3 Solar cell

Solar cells are the device that converts light energy directly into electrical energy through the photovoltaic effect. This process was discovered as early as 1839 and the invention of the first solar cell was reported in 1954 in the Bell Laboratory. The first reported cell was produced on silicon (Si) wafers with a recorded efficiency of 6% using either monocrystalline or polycrystalline crystals. Since then, many solar cells based on CdTe, CdS, CIGS, GaAs, etc., have been reported. The most recent and powerful solar cells in current PV technology are polymer-based solar cells, dye-sensitized solar cells, Si-based solar cells, and perovskite solar cells. Si-based solar cell dominates the current PV market by achieving a high efficiency of 26% in parallel to a modest fabrication cost. The contemporary PV market is dominated by Si-based solar cells because they can achieve a high efficiency of 26% while maintaining a low fabrication cost. Concurrently, a single-junction GaAs-based solar cell achieved an efficiency of 29.3% [2]. The working mechanism and three basic attributes required to operate a solar cell are as follows (**Figure 2**).

i. The generation of excitons or electron-hole pairs upon exposure to light illumination.

ii. The separation of opposite charge carriers toward the respective charge transport layers.

iii. The extraction of dissociated charge carriers to an external circuit of the device.

The energy from the sun to the earth's surface is primarily electromagnetic radiation, which contains a spectral region from 0.3 to 3.0 μm. This spectral region corresponds to the wavelength ranging from ultraviolet to near-infrared. The radiation reaching the earth is scattered and absorbed and the intensity of absorbance depends on the incident angle of radiation. Depending on this latitude, the energy value at the

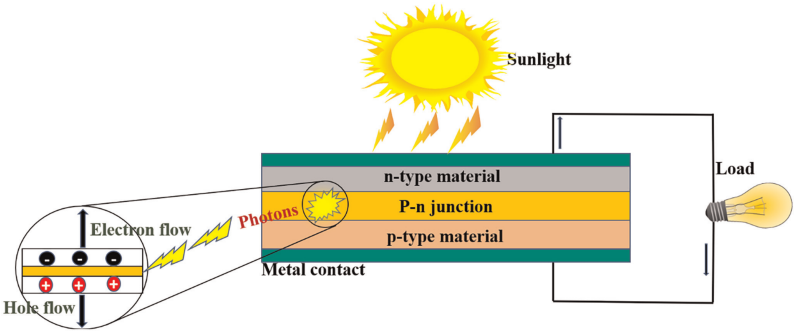


Figure 2.
Working principle of a solar cell.

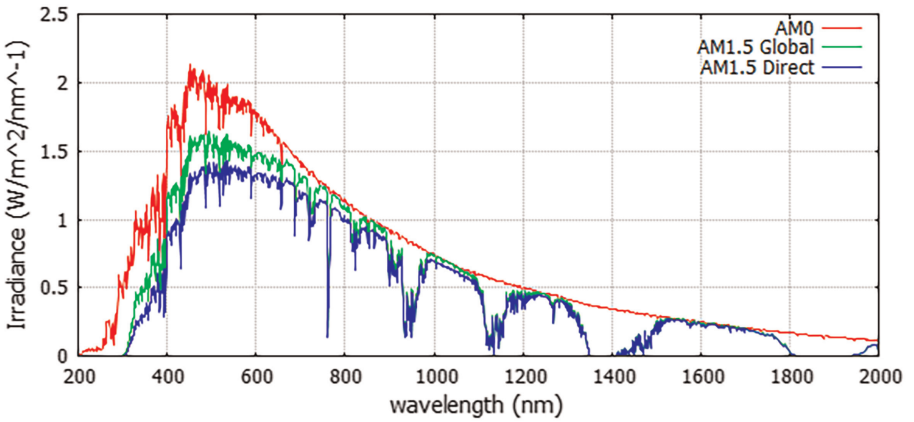


Figure 3.
Standard solar spectrum. (Source: https://www.solar-simulator.info/solar-simulator-match.html).

earth's surface is 1000 W/m^2. The power level outside the earth's surface is about 140 mW/cm^2, which is termed the air-mass-zero (AM0) spectrum. At sea level, with the sun at its zenith, the power level is reduced to 100 mW/cm^2, which is termed AM 1.5G solar radiation (**Figure 3**). The conversion of energy into electricity or spectral response by the solar cells is maximum at this spectral range. The spectral response is the ratio of incident energy to the total conversion of electricity by solar cells. PV technology's primary goal is to increase solar energy absorption in order to produce more power in a more cost-effective, environmentally friendly, and efficient manner.

1.4 Perovskite semiconductor

In 1839, Gustav Rose first discovered $CaTiO_3$, calcium titanium oxide perovskite mineral, in the Ural mountain and is called after Lev Perovski, a mineralogist. Broadly speaking, an assortment of substances termed perovskite crystal structure if it has a crystal structure that is comparable to that of $CaTiO_3$, which has the general formula ABO_3, which was first discovered in 1926 by Victor Moritz Goldschmidt while working on tolerance factor [3]. Goldschmidt defined the first description of the tolerance factor (t), which is an indicator of the stability and distortion of the crystal structure [3]. In a perovskite crystal structure, if a large number of stable metallic elements are present, then t is in the range of 0.75 to 1.

As one of the most abundant structural families, perovskites are found in an enormous number of compounds that have wide-ranging intriguing properties like ferroelectricity, superconductivity, charge ordering, magnetoresistance applications, and importance [4]. The first halide perovskite crystal structure based on cesium (Cs) and lead (Pb) was reported in $CsPbX_3$ by C.K. Moller in 1958 in his study of photoconductivity of the perovskite materials [5]. Tin (Sn)-based halide perovskite was first introduced as conducting channels for the thin-film field-effect transistor more than 20 years ago and in 2012, it was used as the light absorber layer in PSCs [6].

1.5 Properties of perovskites

Perovskite material showed outstanding photovoltaic properties like tunable bandgap, excellent thermal stability, long electron-hole diffusion length, high

absorption coefficient, high charge carrier mobility and transportation, low processing temperature, lower binding energy, and easy processing steps. These basic characteristic properties of perovskite materials make them suitable for a wide range of applications in the field of PV technology. The family of metal halide perovskite crystals adopts a general chemical formula ABX_3. In which, A and B are two different size cations, often A atoms are larger than B atoms and X is an oxide or anion bonds with the other two cations. Additionally, A is monotonic and B is a divalent metal cation [7].

Halide perovskite is of two types: (i) all-inorganic halide perovskite and (ii) mixed or hybrid organic-inorganic halide perovskite. In pure halide perovskite, A refers to Cs^+, B refers to Pb^{2+}, Sn^{2+}, Ge^{2+}, etc., and X can be usually of halide group Cl^-, Br^-, I^-, etc. While in a mixed or organic-inorganic halide group of perovskite, A can be CH_3NH_3, MA^+, FA^+, etc., and X can be a mixture of Cl^-, Br^-, and I^-. In an ideal cubic perovskite crystal structure, "A" cations are positioned at (0, 0, 0) in the cube's corner and are 12-fold coordinated by halogen anions, whereas the halogen atoms "X" are located at position (1/2, 1/2, 0) in the cubic lattice's face center, and tetravalent "B" cations, on the other hand, are octahedral and occupy the location of the body's center (1/2, 1/2, 1/2) [8]. The oxide and halide perovskite can be found in different phases of crystal structure cubic, tetragonal, and rhombohedral depending on the tolerance factor and processing temperature (**Figures 4** and **5**).

The tendency to form the perovskite and non-perovskite crystal phase depends on the formula of the tolerance factor, which is as follows [10]:

$$t = \frac{R_A + R_X}{\sqrt{2}(R_B + R_{X)}} \tag{1}$$

Where R_A = radius of A cation; R_B = radius of B cation; and R_x = radius of X anion.

In general, the tolerance factor (t) can lie between 0.89 and 1 for oxide perovskite and halide perovskite, it may vary from 0.89 to 1.11. The optimal cubic phase of

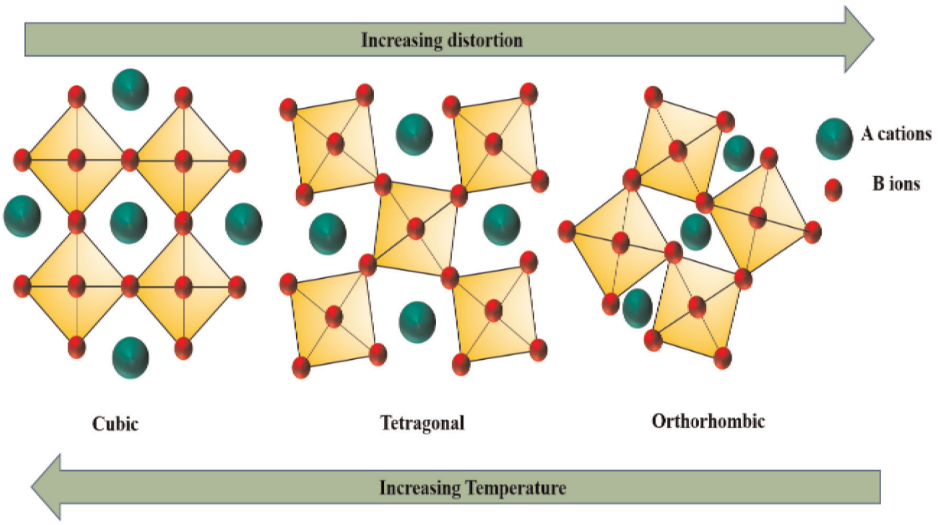


Figure 4.
The phase distortion from cubic to orthorhombic crystal phase V, the temperature, 2D diagram of $CsPbBr_3$ perovskite material.

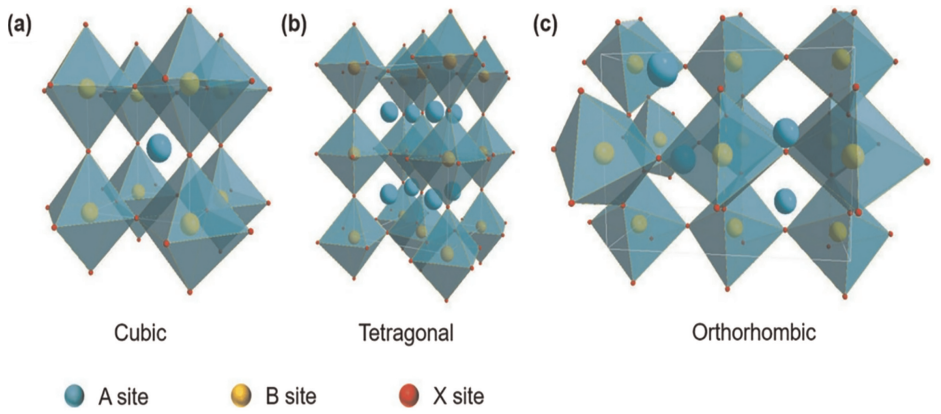


Figure 5.
The phase distortion from cubic to orthorhombic crystal phase 3D diagram of $CsPbBr_3$ perovskite [9].

perovskite is characterized by a t value of 0.8 to 1.0; bigger (>1) or lesser (<1) values of the t factor typically lead to non-perovskite structures [10]. The orthorhombic crystal structure is formed when $t < 0.8$, while a greater value of $t > 1$ gives a hexagonal phase. The ideal cubic structure tends to form a tolerance factor between 0.8 and 1. For a lower processing temperature, an orthorhombic crystal phase is obtained while a lower processing temperature gives a cubic crystal structure. The following trend of tolerance factor is defined for oxide perovskites, but it is still valid for halide groups of perovskites. Hence, the tolerance factor can be considered a reliable empirical index to predict the stability and preferentially formed stoichiometry of perovskite materials [10].

The direct bandgap perovskites have drawn much attention from researchers in photovoltaic applications from solar cells to light detectors and LEDs due to their excellent optical properties like broad absorption ranging across the whole visible spectrum, light absorption coefficient, and tunable bandgap which can be considered as one of the best and promising candidates to replace the Si technology.

To harvest solar energy, the light absorber layer of a PSC is the essential part. The high absorption coefficient of order 10^5 cm^{-1} and broadened absorption window covering ultraviolet to long-range spectrum at a lower thickness of the light absorber layer reduce the fabrication and experimental cost of the device in PSC. The thickness of the perovskite layer in PSC is relatively low in comparison with dye-sensitized solar cells. This may encourage the development and commercialization of PSC at a low cost.

According to Shockley and Queisser (SQ) limits or detailed balance calculation, the maximum power conversion efficiency from a single-junction solar cell is 30% for a single-junction solar cell with a bandgap of 1.1 eV of light-absorbing materials; however, the current calculation increased the efficiency to 33.16% at a bandgap of absorber layer 1.34 eV (**Figure 6**).

Despite this SQ calculation, the single-junction solar cell can hardly touch the upper limits. Other than the bandgap of the absorber layer, various factors like defect level, interfacial defects, doping concentration, vacancies, and interstitials limit the theoretical maximum efficiency. Out of 100% of solar energy, only 33% was converted into consumable electricity, and out of the remaining 67%, 47% was

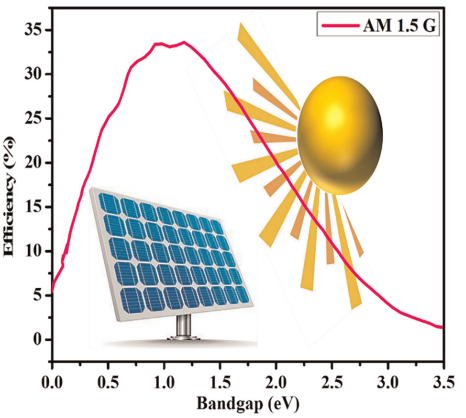


Figure 6.
Shockley and Queisser limits [11].

converted into heat, 18% was transmitted through the cell, and 2% was lost from the local recombination process of charge carriers.

The broad tunability of compositional choices upon the main three components of perovskite A, M, and X can lead to a variety of perovskites with different optical properties, which allow us substantial flexibility in choosing suitable perovskite material for specific optoelectronic applications (**Figure 7**) [12–14].

The tunable bandgap of perovskite materials enables efficient absorption of light and produces large excitons in a light-emitting gadget or photovoltaic device when exposed to light. The bandgap of perovskite materials can be easily adjusted by merely altering the halides' mixing ratio (Br-Cl, I-Br, etc.) [15]. The tunability of the bandgap of perovskite allows the creation of multicolor light-emitting devices and any specific required device. Hence, compositional engineering can give an easy path to obtain the desired optical property, which sufficiently enlarges the absorption window of perovskite material to utilize solar energy.

The perovskite material exhibits outstanding electrical properties such as conductivity, excitons binding energy as low as 2 meV [16], charge carrier mobility >100 cm^2V^{-1} s^{-1}, the diffusion length of electrons and holes exceeding 150 μm [17],

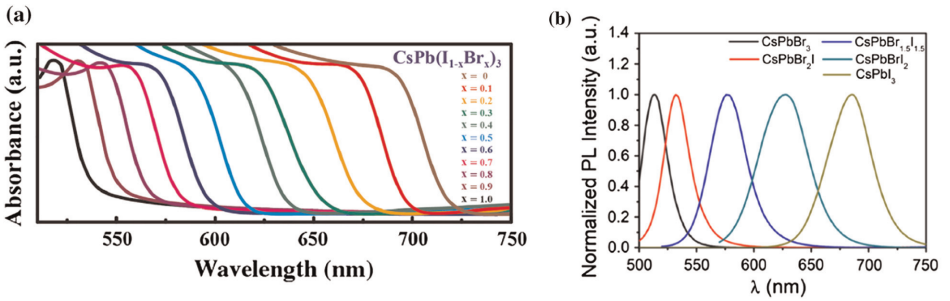


Figure 7.
Bandgap tuning of inorganic perovskite material by compositional engineering method (a) Absorbance spectra for inorganic perovskite films of different nanocomposites, $CsPb(I_{1-x}Br_x)_3$ Reprinted with permission from Ref. [12]. Copyright 2022, Elsevier B.V. (b) PL spectra of the $CsPbI_3$, $CsPbI_2Br$, $CsPbI_{1.5}Br_{1.5}$, $CsPbIBr_2$, $CsPbBr_3$ films. Reproduced with permission [13]. Copyright 2022, Elsevier B.V.

photoluminescence quantum yield (PLQY), low trap density of states 1E+10 cm^{-3} [18], and photoresponse as compared to the crystalline silicon [19]. Also, a unique property of this material is the ability to both act as a light-absorbing material and as a charge carrier transporter [20].

The mobility of charge carriers helps to determine the performance of the semiconducting materials in optoelectronic applications. In general, the electron mobility is comparatively higher than the hole mobility since the effective mass of electrons is smaller than the holes. The holes function within the tightly bound valence band rather than the conduction band, which slows the movement of holes inside the potential well of semiconducting materials. The higher mobility >100 cm^2V^{-1} s^{-1} of charge carriers in perovskite can be utilized in excellent carrier transportation character to improve the performance of perovskite-based cells [17, 21].

The operation mechanism of PSC depends on the fraction of excitons, which are thermally dissociated into free charge carrier electrons and holes upon light illumination on solar cells. PSCs produce a significant fraction of excitons within the perovskite layer depending on the energy bandgap. Perovskite materials reported a very low binding energy of 2 meV as compared to other semiconducting technology silicon [16]. In perovskite, generally two types of excitons are possible: (i) Frenkel excitons, which are tightly bound charge carriers that cannot move outside the unit cell, and (ii) Wannier excitons, which are weakly bound charge carriers free to move in the perovskite crystals. Wannier-Mott excitons are generally expected in the perovskites, which are often described in terms of the hydrogen model [22]. The binding energy depends on the temperature and it decreases at higher operating temperatures.

The average travel distance before the recombinations of charge carriers in perovskite crystals is significantly higher >150 μm and therefore the longer lifetimes of charge carriers [17]. The growth of perovskite microcrystals and rods provides a longer diffusion length of charge carriers. The lifespan and diffusion length are interconnected to each other as the higher diffusion length more the carrier's lifetime which is beneficial for the optoelectronic device. The diffusion length and lifetime of electrons and holes also depend on the defect density of the absorber layer; the higher defect level of the absorber layer limits the lifespan and diffusion length of charge carriers.

The acquisition of extreme thermal properties in perovskites has become more and more important because both the lifetime and performance of the device are majorly influenced by the temperature or temperature gradient [23]. Metal halide perovskite, $CsMX_3$, has excellent thermal stability, conductivity, and heat dissipation as compared to other organic perovskites (**Figure 8**) [23]. The various morphologies of perovskites

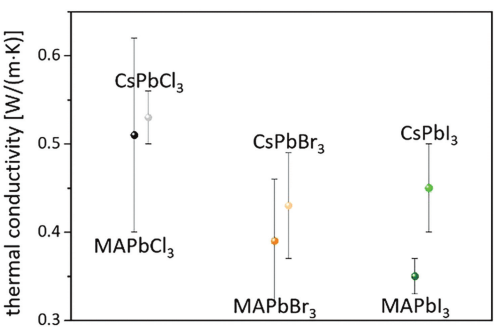


Figure 8.
Comparatively higher thermal conductivity in $CsMX_3$-based perovskites [23].

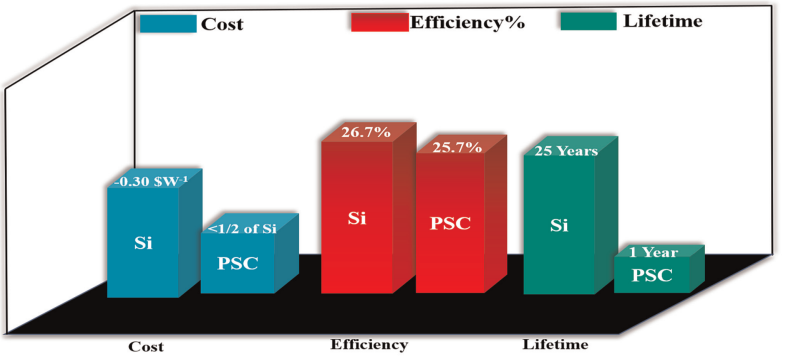


Figure 9.
Comparison of perovskite and silicon solar cells on golden triangle cost, efficiency, and lifetime. Si solar cells have a champion efficiency of 26.7% and a lifetime of over 25 years at a cost of around 0.3 W^{-1} [26]. In comparison, PSC achieves an efficiency of 25.7% and a lifetime of 1 year at a cost of half of the silicon solar cell [25].

like micro-rods and the phase transformation to a stable phase reduce the rate of endothermic and exothermic reactions, which improve the self-thermal stability of the device [24].

The perovskites gained huge interest from experimenters due to the low cost of raw processing materials, which are half of silicon solar cells, higher efficiency up to 25.7% [25], and durability of around 1 year (**Figure 9**). However, currently, silicon solar cells achieve an efficiency of 26.7% and can operate over 25 years for the cost of 0.3 $\$W^{-1}$ [26]. Despite the higher efficiency of silicon solar cells, it is a very complex and lengthy process to extract Si from sand to Si wafer. Si technology is an expensive, high-energy process, generating a high level of waste material and is time-consuming. On the other hand, in a very convenient, easy processing way simpler, lower cost, lower embodied energy, and massively reduced environmental impact PSC can be produced and run. The large area role-to-role fabrication of inorganic $CsPbBr_3$, $CsPbI_3$, $CsPbI_2Br$, etc., perovskite thin film does not require any special processing environment. However, organic perovskites like $MAPbI_3$, $CH_3NH_3PbI_3$, $FASnI_3$ are very sensitive to moisture and oxygen present in the external environment and require inert (Nitrogen) processing conditions.

1.6 Perovskite solar cells

A perovskite solar cell (PSC) is a device that converts the photons of light from the sun into usable electricity.

A perovskite solar cell is made of three main parts:

i. Light-harvesting layer: a lead or tin-halide-based perovskite or semiconducting layer that acts as the light-harvesting active layer and converts the incident photons into electrons and holes [27]. Examples: all-inorganic perovskite—$CsPbBr_3$, $CsPbI_2Br$, $CsPbBr_2Cl$, $CsSnI_3$, alloy-based perovskite—$CsPb_{0.75}Sn_{0.25}I_2Br$, etc. The perovskite layer is sandwiched between the carrier collector layers as an active layer. The built-in electric field is generated in the perovskite and is due to the contact difference of potential between the ETL and HTL.

ii. Carrier collector layers: the p-type hole transport layer (HTL) and n-type electron transport layer (ETL) act as carrier collector layers that extract holes and electrons, respectively, from the perovskite layer. If the conduction band Ec and valence band Ev of both of the semiconducting materials lie below the Ec and Ev of the absorber layer, it will work as ETL and the opposite for HTL. Examples: ETLs-ZnO, TiO_2, GO, CdS and HTLs-Cu_2O, MoO_3, P3HT, etc.

iii. Metal contacts: The metallization layers on either side of the ETL and HTL layers act as electrical accessing electrodes and transfer the carriers to the circuit. If the work function of metal contact lies below and close to the conduction band of ETL or above the valence band for HTL, it will act as an electrode. Examples: C, Au, Ag, Cu, etc. The surface of PSC is coated with an anti-reflection coating to avoid the loss of incident light energy due to reflection. Also, to avoid external exposure of PSC to moisture and oxygen, PSC is encapsulated.

1.7 Working principle of perovskite solar cells

The working principle of PSC is based on the photovoltaic effect. The photogeneration of charge carriers in the light active layer is a result of the absorption of light radiation. When the photon hits the PSC, the active layer absorbs the solar energy and becomes a hotspot of the charge carriers. These charge carriers are loosely bound like metallic semiconductors, for example, silicon. Furthermore, the generated electrons dissociated toward the ETLs and holes dissociated toward the HTLs, which are extracted by the respective electrodes to the circuit, hence generating external electricity. The electricity is further amplified by using an inverter for different optoelectronic applications, **Figure 10**.

1.8 Thin-film perovskite solar cells

Thin-film perovskite solar cells are second-generation solar cells. In the thin-film solar cell, the thickness of the absorber, ETL, and HTL layer is in scale from a few nanometers (nm) to tens of micrometers (μm), which is much thinner than the rival technology: the first-generation crystalline silicon solar cell which has silicon wafers of

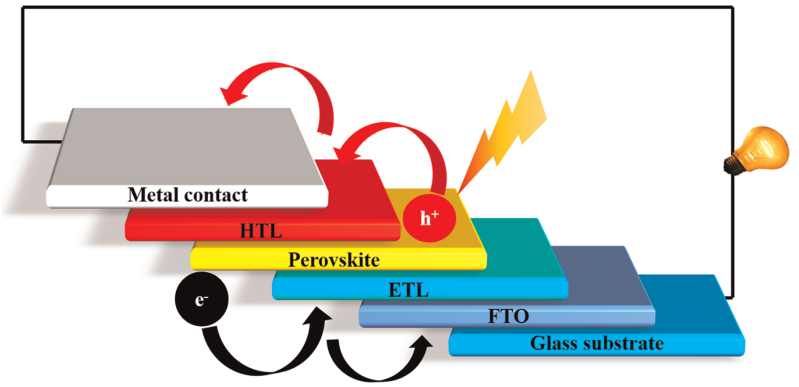


Figure 10.
Working principle of a PSC.

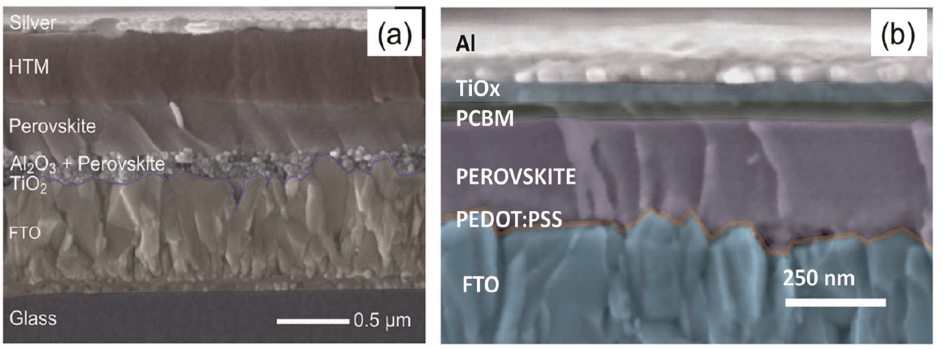


Figure 11.
(a) Cross-sectional SEM view of thin-film architecture-FTO/TiO_2/$Al2O_3$/Perovskite/HTM/Ag in the range μm. (b) cross-sectional view of a planar perovskite solar cell FTO/PEDOT: PSS/Perovskite/PCBM/TiO_x/Al in the range nm [28].

the thickness of 200 (μm) (**Figure 11**). The thin-film solar cell can be fabricated by depositing one or more thin layers on top of others. The powder of perovskite dissolves in the desired solvent to prepare a precursor solution for thin-film coating on top of a glass substrate, which is generally Fluorine-doped Tin oxide (FTO), in an extremely easy way. Further solution-coated wet film followed by drying and annealing to get the thin layer of solar cells. One of the most important advantages of thin-film solar cells is that they can be fabricated as flexible devices. The integration architectures of the flexible device with mass reduction have shown great potential in the field of wearable power supply due to flexibility, lightweight, portability, and compatibility without violating the actual function of the PSC [29].

2. Factors affecting the performance of perovskite solar cells

The performance of the PSC is affected by various photovoltaic parameters like bandgap of the absorber layer, type of ETL and HTL materials, and their thickness, interfacial recombination, series resistance, defect level of the absorber layer, and working temperature.

2.1 Bandgap

The active layer of the solar cell is a semiconductor that has a conduction band (CB) and valence band (VB). The gap between the CB and VB is termed as the bandgap of semiconducting materials. The conductors have no bandgap, semiconductors have bandgap smaller than 3 eV, and insulators have bandgap larger than 3 eV (**Figure 12**). The main reason for using semiconducting materials in solar cells is that sunlight excites the electrons from the CB to VB.

For insulating materials, solar energy is insufficient to excite the electrons to higher energy levels. There is an abundant source of semiconducting materials that have light-absorbing properties, which can be utilized in solar cells to generate power. In a semiconductor, photons with energy equal to or higher than the bandgap energy can lead to the absorption of light and produce excitons in the semiconductor [22]. Several mechanisms like the addition of impurity or compositional engineering of the

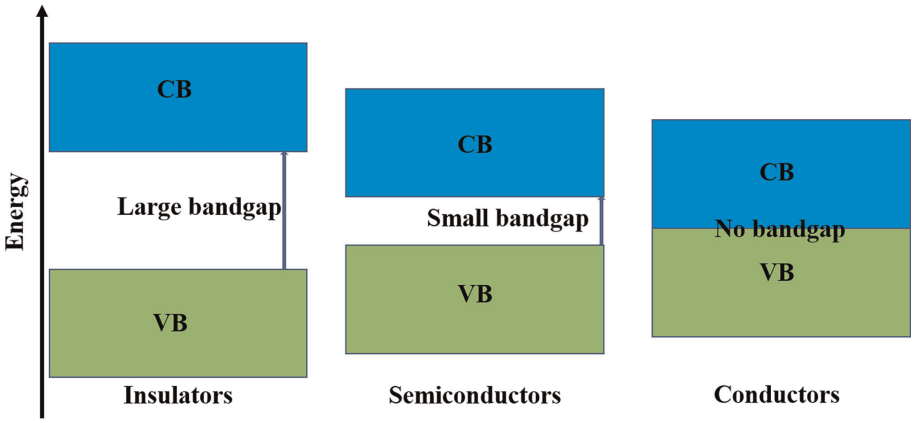


Figure 12.
Schematic diagrams of the energy band of insulator, semiconductor, and conductor.

base material can tune the bandgap and facilitate a higher PCE. Semiconductors are both direct and indirect materials and with the help of Tauc's equations, their bandgap can be calculated conveniently [30].

$$(\alpha h\upsilon)^n = k\left(h\upsilon - E_g\right) \tag{2}$$

Where h = Planck's constant; α = absorption coefficient; E_g = bandgap energy; k = proportionality constant; hυ = photon energy; n = 2, 1/2 for direct and indirect bandgap materials, respectively. In general, the relation between open-circuit voltage Voc and the band gap of the semiconducting material can be illustrated by the following equation:

$$V_{OC} = \frac{E_g}{q} - \frac{nKT}{q}\, log\left(\frac{J_{SC}}{J_0} + 1\right) \tag{3}$$

Where q = charge carriers; k = Boltzmann's constant; J_{SC} = short-circuit current; J_0 = reverse saturation current density; T = temperature; and n = ideality factor.

The Voc value of a solar cell will always be below the bandgap of the given materials, as the Voc is limited by the bandgap as shown in Eq. (3). The lower Voc in PSC is due to the recombination and non-radiative transitions of charge carriers. A Tin-based perovskite material overcomes the Voc loss by lowering the bandgap by adding the dopant of rubidium iodide (RbI) and potassium iodide (KI) in a tin-lead (SnPb)-based absorber and achieving a PCE of 21.04% (**Figure 13**) [9]. However, besides the bandgap, the stoichiometry, structures, and morphology differ from material to material, hence impacting the device's performance and possibilities for PV applications. A device with higher power conversion efficiency, low cost of raw materials, low consumption of processing energy, simple device production steps, and low price can be considered an excellent device.

2.2 Choice of ETL and HTL materials

Each functional layer of the PSC, absorber, ETL, and HTL layer plays a very important role in the photovoltaic performance of the device. When perovskite is

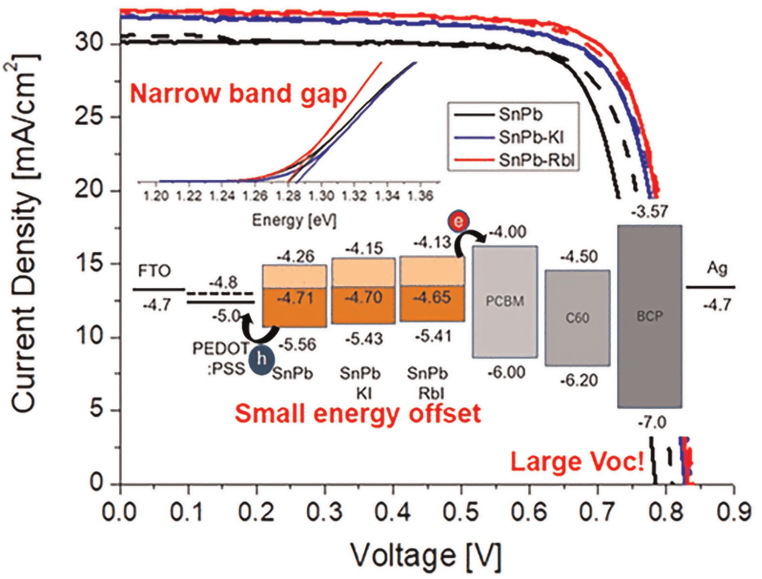


Figure 13.
A Tin-based PSC showed higher efficiency when tunning the bandgap. Reproduced with permission [9]. Copyright @ 2022, American Chemical Society.

structured with the various ETLs and HTLs materials, a mismatch between the energy level has risen due to the difference in the highest occupied molecular orbital (HOMO) and lowest unoccupied molecular orbit (LUMO) of functional materials. This discontinuity in the energy level of different materials gives the energy level diagram (**Figure 14**) [31]. The energy difference between the vacuum level and the conduction band minimum is provided by the electron affinity. The bandgap or the energy difference between the valence band maximum and the conduction band minimum is given by the symbol E_g. The energy bandgap and electron affinity values of each semiconducting material vary. The band diagram is positioned with the electron affinity of HTL, $CsPbBr_3$, and ETL layer (**Figure 14**). The energy level mismatch

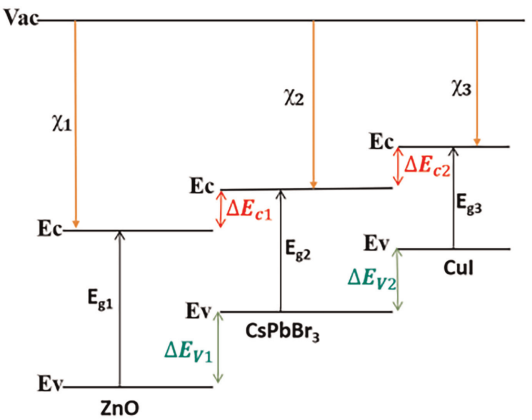


Figure 14.
Band diagram positioned with the energy bandgap and the electron affinity of HTL, $CsPbBr_3$, and ETL layer.

between the ETL/perovskite and perovskite/HTL causes a discontinuity at the interface, where the ETL-ZnO, perovskite-$CsPbBr_3$, and HTL-CuI come together. Note: in this diagram, we assume a constant Fermi energy level.

In **Figure 14**, x_1, x_2, and x_3 are the electron affinity of ETL-ZnO, perovskite-$CsPbBr_3$, and HTL-CuI, respectively. The conduction band and valence band energy are represented by Ec and Ev, respectively, while Vac is the vacuum level. E_{g1}, E_{g2}, and E_{g3} are the bandgaps of ETL, absorber, and HTL layers, respectively. The discontinuity is given by the following equations:

$$\Delta E_C = x_1 - x_2 \tag{4}$$

$$\Delta E_V = \left(x_1 + E_{g1}\right) - \left(x_2 + E_{g2}\right) \tag{5}$$

Where ΔE_c is the negative value representing the difference in the semiconductors' electron affinities. ΔE_V, which is a positive amount according to Anderson's law, is the sum of the differences in bandgaps and electron affinity [32, 33]. The discontinuities, or conduction band offset (CBO), at the ZnO/$CsPbBr_3$ and $CsPbBr_3$/CuI interfaces, are represented by ΔE_{C1} and ΔE_{C2}, respectively, and are caused by the misalignment of the energy levels. The discontinuity's minimal optimal value, $\Delta E_c \sim (-0.2\ \text{eV})$, the discontinuities at the ZnO/$CsPbBr_3$ and $CsPbBr_3$/CuI interfaces are denoted by ΔE_{V1}, ΔE_{V2}, and VBO, respectively. 0.1 eV is the minimum value of ΔE_V. Positive conduction band offset occurs when ZnO's conduction band is lower than the $CsPbBr_3$ absorber layer's. It serves as a barrier to prevent electrons from moving backward from ZnO to the $CsPbBr_3$ layer. Conversely, a negative conduction band offset (CBO < 0) occurs when the ZnO conduction band is larger than the $CsPbBr_3$ layer's [34]. Because the backward flow of electrons cannot be sufficiently stopped by the negative CBO, charge carrier recombination takes over. In heterostructure solar cells with n-i-p, this conduction band offset occurs. Similar to a p-n junction solar cell, a depletion layer forms to cause band bending E_{F1}-E_{F2}, as both the hole and the electron move from the p- to the n-region and from the n- to the p-region, respectively. The n-i-p heterostructure device and p-n junction device are identical [35]. The device's permittivity, doping, and relative Fermi level all have a significant impact on the band bending value. As a result, we can adjust the CBO and VBO between the materials to raise the efficiency to a higher value by selecting different basic materials for the PSC.

Also, we are free to combine the different HTLs and ETLs materials with the perovskite layer, based on different factors like cost, nature of materials, alignment with the absorber layer, sintering temperature, lattice constant, etc. It is very easy to process an ETL-TiO_2 for PSCs, but its major drawback is requiring a high sintering temperature of 500°C and having very low mobility (0–0.1 $cm^2V^{-1}\ s^{-1}$) and low UV-stability [36]. To overcome this shortcoming, many other n-type metal oxide semiconductors like ETL- ZnO, SnO_2, GO, WO_3, $ZnSO_4$, CdS (**Figure 15**) can be replaced by TiO_2 [34, 37]. ZnO is an inorganic and low-cost material and it improved the stability of the device. Similar to the deposition of the perovskite layer, it is very easy to deposit the ETL layer on the glass electrodes. The choice of different materials may be appropriately aligned with the perovskite and give higher PCE from the device by reducing the total rate of recombination of charge carriers (**Figure 16(a)** and **(b)**). The higher CBO at the interface dramatically influences the current density V_s voltage curve (**Figure 16(d)**). Tunning the electron affinity of ETL and HTL materials to match the energy alignment with the absorber layer is another way to push the

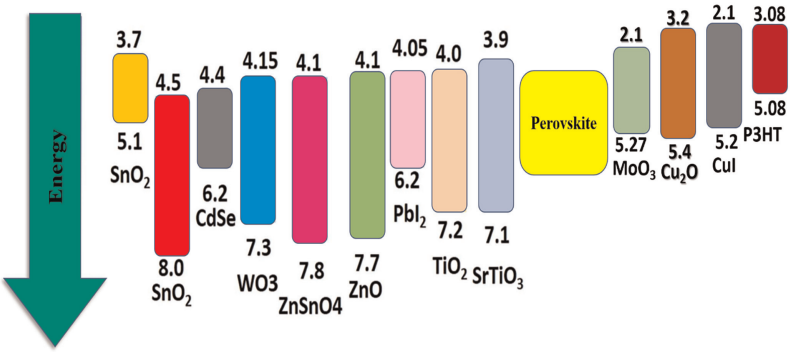


Figure 15.
Various choices of cost-effective ETL and HTL materials can be aligned with perovskites.

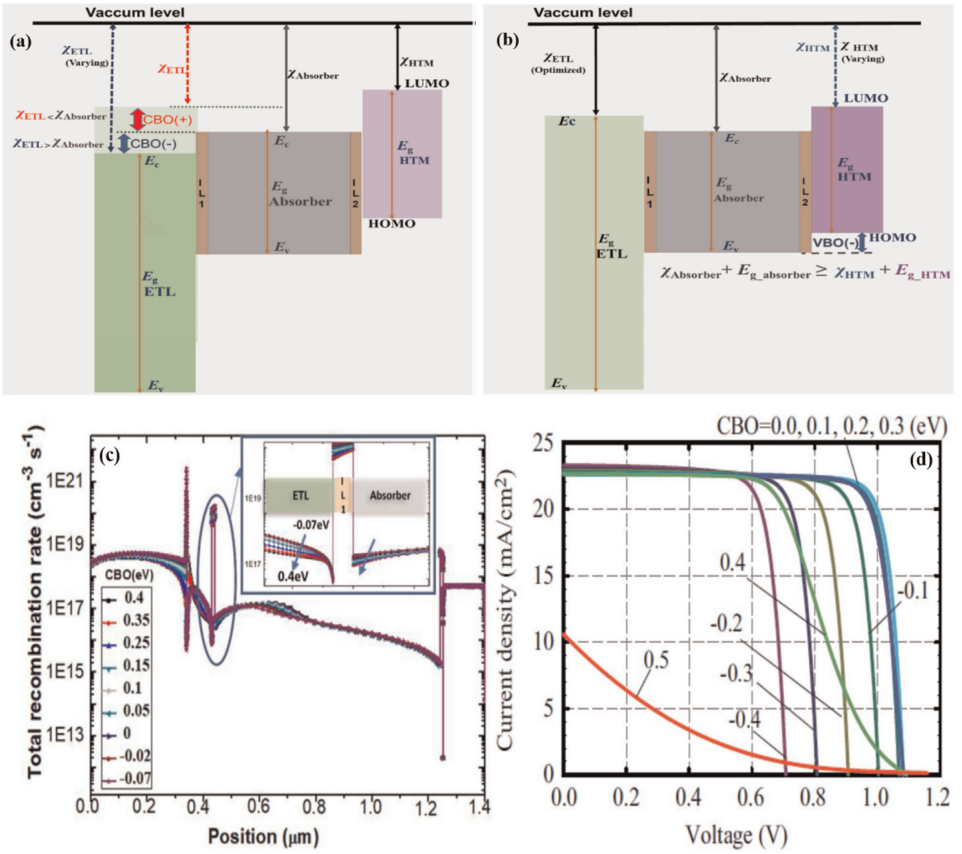


Figure 16.
(a, b) Formation of CBO and VBO at the interface ETL/perovskite and perovskite/HTL, respectively, (c) reduction in total recombination of charge carriers at interface ETL/perovskite and influence of CBO on (d) current density Vs voltage curve. Reproduced with permission [34]. Copyright 2020, Elsevier B.V.

efficiency of the device to a higher extent at a lower cost and with experimental wastage. Yassine et al. achieved a higher PCE of 25.21% by modulating the CBO of SnO_2 with the perovskite layer (**Figure 16(c)**). Similarly, in place of high-cost

Spiro-OMeTAD, the various p-type HTL materials like CuI, Cu_2O, MoO_3, P3HT, NiO, can be used for low-cost, high hole mobility and easy in-processing materials, which can fasten the extraction of the holes from the absorber layer.

2.3 Thickness of perovskite, ETL, and HTL materials

The thickness of the perovskite, ETL, and HTL layers is one of the most important parameters to enhance the performance of the device. Because of its effect on the electron and hole diffusion length of the charge carrier, the thickness of the absorber layer directly affects the solar cell's performance. As it is known, for an absorber layer with minimal thickness, the rate of light absorption is very low, which results in low photocurrent due to enhancement in carrier's recombination, hence reducing the device functionality. Conversely, a very high thickness of the absorber layer may not give an appropriate diffusion length to the charge carriers to travel toward the charge transport layers ETLs and HTLs; consequently, the recombination of charge carriers in the perovskite layer gives the low performance of the device [38]. As such, to enhance the performance of the solar cells, the thickness of the absorber layer needs to be not very thick or thin. The photovoltaic parameters like Voc, Jsc, Fill factors (FF), and PCE of the device are very much influenced by the thickness of the perovskite layer. The series resistance of the device is related to the bulkiness of the device; hence, a thin layer of perovskite also reduces the series resistance of the device, which helps to improve the PCE.

Similar to the thickness of the absorber layer, the thickness of the ETL and HTL layers in PSC also influences the performance of the device. The charge transport layers of PSC are the central part of the solar cell. The illumination falls on the absorber layer converted into excitons. Consequently, the electrons and holes are extracted by ETL and HTL layers, respectively. Furthermore, the separated charge carriers move toward the respective electrodes and in the external circuit through metal contact. However, it is important to fully cover the perovskite layer with HTLs for the dissociation of holes toward the electrode. The charge transport layers are responsible for the transportation of generated charge carriers from the absorber layer. Thus, the thickness of ETL and HTL layers can impact the production rate of charge carriers, their transportation, and the performance of the device. For a thin HTL layer, the holes travel a shorter distance toward the electrodes and reduce the probability of recombination; hence, the ideal thickness of the HTL layers should be in the range of 100–200 nm to fully cover the perovskite layer and for better performance of the device [39]. The thick ETL layer creates the bulkiness of the device, hence increasing the series resistance of the device. Therefore, it is critical to determine the proper ETL and HTL layer thickness in order to cover the crystallites without compromising the device's series resistance.

2.4 Defect density of perovskite

The photovoltaic actions like absorption of photons, carrier generations, and transportation process take place in the absorber layer. Hence, the absorber layer is the core of PSC. The quality and morphology of perovskites influences the performance of solar cells as they impact the lifetime of charge carriers and the rate of generation/recombination of electrons and holes [38]. The defect density of the absorber layer is a crucial parameter that needs to be a concern for the enhancement of the performance of the device. The defect in the perovskite layer majorly occurred due

to poor morphology and non-uniform coverage of the perovskite on the glass substrate leading to the formation of vacancy and voids/pinholes. The defect in the absorber layer causes the direct linkage of perovskite with the ETL and HTL layer and enhances the recombination rate of electrons and holes that limit the overall performance of the device [40]. The defects in perovskite cause electrical instability in the device. Due to the uneven surface and morphology of the perovskite layer, defect levels like interstitial, dislocation, Schottky, and Frenkel defects can exist in between the bandgap of the material, which can eat and trap the electrons that result in non-radiative transitions that highly influence the PCE of the device [41, 42]. If the activation energy is sufficiently small, then trap electrons are likely to be emitted, back to CB (or VB) by phonon absorption. On the other hand, if the activation energy is large, then it is more likely that trapped electrons (or holes) will annihilate or recombine with an opposite charge carrier before it can be emitted [43]. The recombination with the opposite charge carriers can be non-radiative transitions that are assisted by phonon emission [43]. This is an important loss mechanism in PSCs and the rate of recombination is determined by the Shockley-Read-Hall (SRH) mechanism [44].

$$R_{RSH} = \frac{np - {n_i}^2}{\tau\left(p + n + 2n_i \cosh\left(\frac{E_i - E_t}{kT}\right)\right)} \tag{6}$$

$$L = \sqrt{(D \times \tau)} \tag{7}$$

$$\tau = \frac{1}{\sigma \times N_t \times v_{th}} \tag{8}$$

Where E_t = defect energy level; L = diffusion length of charge carriers; N_t = defect density; σ = carriers capture; v_{th} = thermal velocity; D = diffusion length; τ = lifetime of charge carriers; and n_i = electron concentration.

Furthermore, as illustrated in **Figure 17**, the departure from an ideal lattice structure is referred to as a defect that can occur in the perovskite crystal structure in a variety of ways, including vacancy, interstitial, dislocation, grain boundaries, Frenkel,

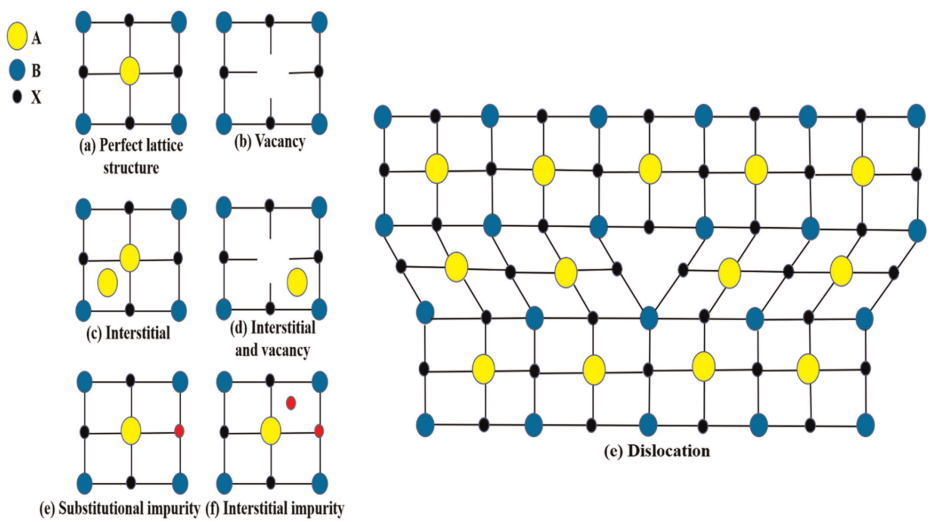


Figure 17.
Types of defects that can exist in perovskite material.

and Schottky defects [43, 45, 46]. These flaws affect exciton extraction, cause instability and non-radiative recombination, and prevent PSCs from being used commercially [46, 47]. Additionally, the literature review demonstrated that the following successful techniques can be used to experimentally reduce the absorber layer's defect density and increase the device's efficiency:

i. The device's stability, defect concentration, and performance are all greatly influenced by the thin perovskite layer deposition technique [46, 48]. Numerous factors, including stoichiometry balance, compound mixing technique, annealing temperature, grain size, solvent, and contaminants from the synthesis environment (such as oxygen and moisture), influence the concentration of defects in the absorber layer [49]. Numerous deposition techniques, doctor blading, chemical bath deposition (CBD), sequential vacuum deposition, including chemical vapor deposition (CVD), and spin-coating (one-step and two-step deposition), have been used for the synthesis of the perovskite layer for large area role-to-role fabrication were employed to create the perovskite layer for large-scale role-to-role manufacturing [46, 50–52]. Enhanced efficiency in the CVD process and one-step spin-coating deposition, compared to the two-step deposition approach, was demonstrated by Azat Akbulatov et al. Additionally, the step deposition method produces a quick nucleation process of perovskite film with a decreased root mean square (RMS) roughness, which results in a smoother, less imperfect, and pin-hole-free PSC light active layer [46, 53].

ii. Increasing the perovskite layer's grain size results in a low trap density of states, increased thermal stability, and less charge carrier recombination, all of which enhance the device's PCE [54, 55]. Moreover, the processing temperature and crystallization rate have a significant impact on grain size; large grains can be produced by gradually lowering the temperature [46, 47, 56–58].

iii. The thermally treated perovskite film, indicating a defect-free perovskite surface in PSC, has a lifespan of charge carrier recombination longer than 7 μs, [54].

iv. Perovskite thin-film doping and compositional engineering techniques can greatly reduce the status of the trap of the material, improving device efficiency by passivating defects and lengthening the charge carrier recombination lifetime [46, 59]. To increase PSC efficiency, the defect density of the perovskite layer can be reduced using a variety of deposition parameters and methods. According to Shoulong Chen et al., the AgBr doping quickly reduced the defect density from 5.059E + 15 cm^{-3} to 3.509E+15, improving the performance of the AgBr-doped $CsPb_{0.99}Ag_{0.01}Br_3$ PSC in comparison with the undoped cell. By lowering the VTFL [46], the addition of a suitable amount of AgBr to the CsPbBr3 film decreased the defect level in the photoluminescence (PL) emission (**Figure 18**).

The value of trap or defect density is given by the formula [59]:

$$n_{trap} = \frac{2\varepsilon\varepsilon_0 V_{TFL}}{qL^2} \tag{9}$$

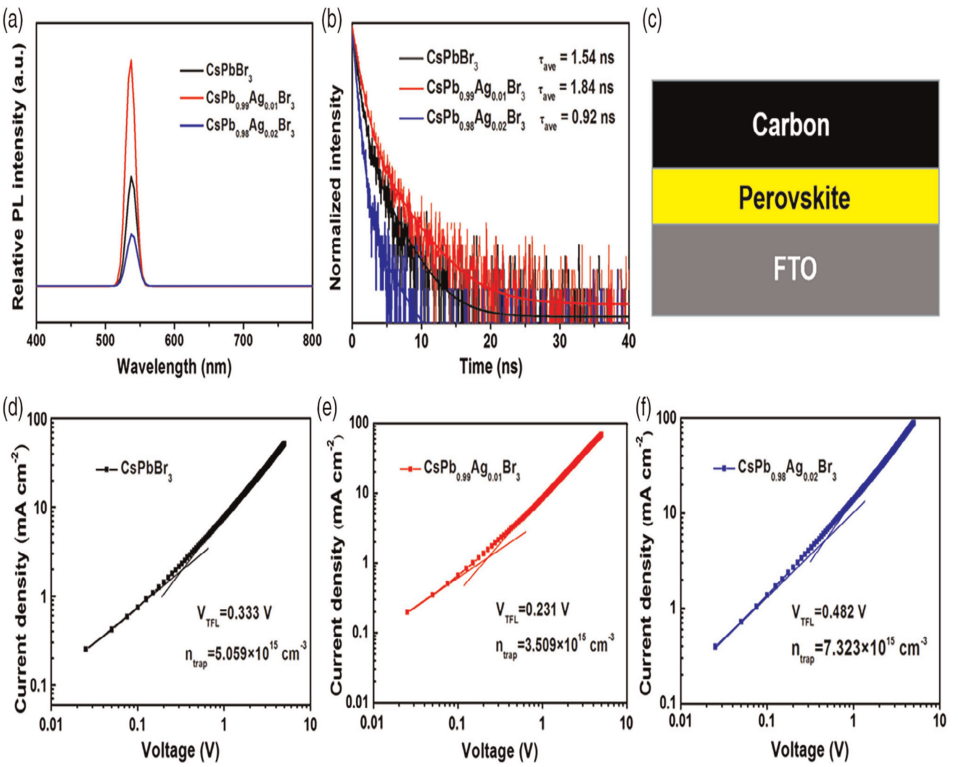


Figure 18.
(a) PL and (b) TRPL spectra for different $CsPb_{1-x}Ag_xBr_3$ (x = 0–0.02) films (c) Dark J-V measurement device structure: FTO/perovskite/carbon (d–f) Dark J-V curves characterization in different perovskite films [59].

Where ε_0 = vacuum permittivity; ε = dielectric constant; L = thickness of the film; V_{TFL} = trap-filled limited voltage.

It is also worth noting that excessing doping may increase the defect level. Hence, the defect level of the light-absorbing layer should be lower as much as possible.

2.5 Series resistance of the device

The performance of the device is significantly affected by the series resistance of the device and the series resistance existence in the device is majorly due to the non-uniform morphology of film, circuit connections, bulk resistance, front and back metal contacts, and defects in perovskite layer [34, 60]. The ETL layer was not covered completely because of the uneven and inadequate quality perovskite layer, which affects the ETL/perovskite interface and increases the contact resistance of the device [61]. The series resistance influences the performance of PSCs. The series resistance of the devices has very little impact on the Voc of the PSC. The major impact of the series resistance is on the FF and PCE of the device [62]. However, excessively high values of series resistance reduce the short-circuit current density (Jsc) of the device. Series resistance does not affect the solar cell at Voc since the overall current flows through the cell. However, near the Voc, the current density V_s voltage (J-V) curve is strongly affected by the series resistance (**Figure 19**).

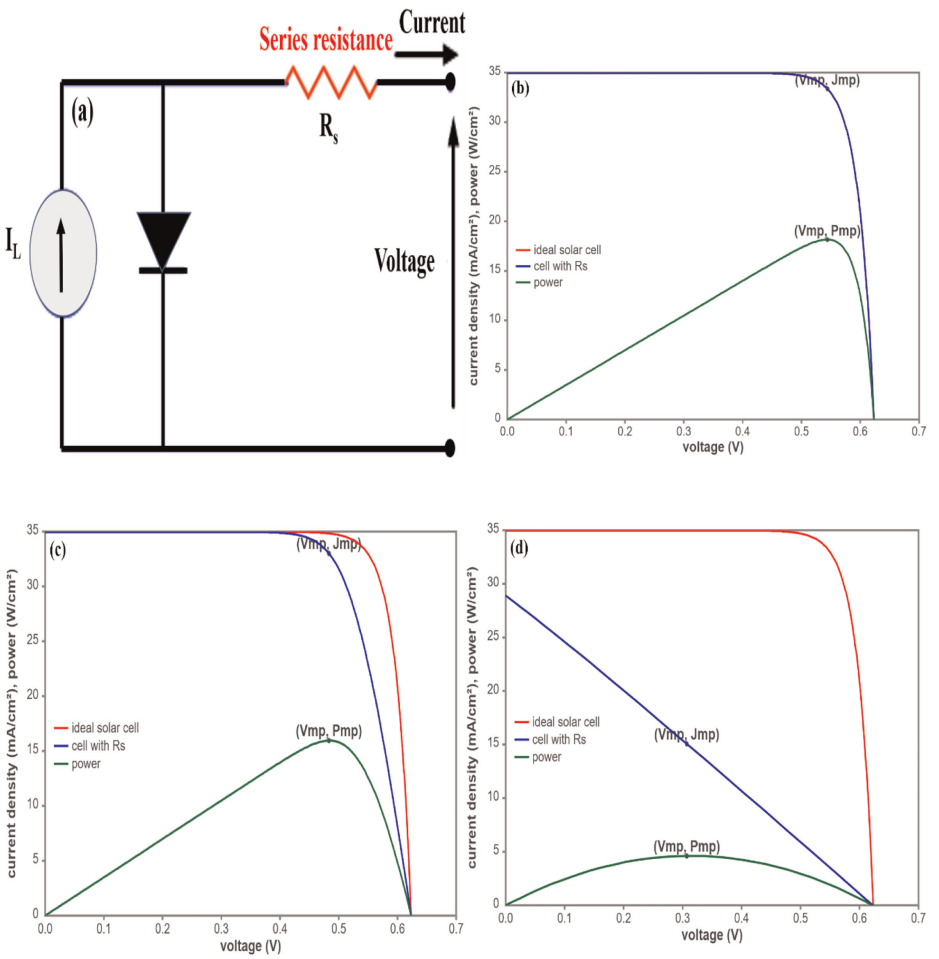


Figure 19.
(a) Equivalent circuit and impact on J-V curve at series resistance (b) 0 ohm.cm² (c) 2 ohm.cm² (d) 20 ohm.cm². (Source: https://www.pveducation.org/pvcdrom/solar-cell-operation/seriesresistance#:~:text=Series%20resistance%20in%20a%20solar,top%20and%20rear%20metal%20contacts).

The straightforward method to estimate the series resistance from the solar cell is to find the slope of the J-V curve at the Voc. The following formulas connect the Voc to Jsc using the device's diode equivalent circuit model [63]:

$$I_{SC} = I_o\left(exp\left(\frac{qV_{OC}}{e^{nKT}}\right) - 1\right) \tag{10}$$

$$I_{SC} = I_L - I_o\left(exp\left(\frac{qV_{OC}}{e^{nKT}}\right) - 1\right) - \frac{V_{oc} + I_{sc}\bullet R_s}{R_{SH}} \tag{11}$$

Where I_{SC} = short-circuit current; T = temperature; I_L = light-induced current; n = ideality factor; k = Boltzmann's constant; R_s = series resistance; and R_{SH} = shunt resistance.

We can see from the preceding calculations that an increase in series resistance has a major effect on the device's Jsc, which lowers the PCE and FF. To achieve the maximum PCE from the device, the series resistance of the device should be lower as much as possible. We must investigate and explore the configuration and use of the raw materials for the PSC, which have naturally lower series resistance like HTL-free configuration and carbon (C). HTL-free configuration of the cell lowers the bulkiness and contacts of the device, hence reducing the series resistance of the device. As a result, the device's defect level, film shape, series resistance, and film quality all contributed significantly to its efficiency.

2.6 Operating temperature

The operating temperature has a great impact on the performance of the PSCs. Perovskite materials are very sensitive to temperature and since the solar cells are implanted in the outdoor environment, it is very important to study how temperature can affect the device. The photovoltaic cells are operated under direct sunlight and therefore by the sun's heating, the cell temperature can be higher than 45°C, which is higher than the normal environment temperature [64]. Given the synthesis process of the PSCs, perovskites show three crystal phases, α, β, and γ, depending on the processing and crystallization temperature [64]. When processed at a higher temperature, the perovskite starts to decompose to constitute perovskite. However, sometimes the temperature-dependent processing method like the slow-lowering temperature method may be beneficial for the effective growth and crystallization of perovskite.

The stability of PSCs at the higher operating temperature is a critical challenge in the field of commercialization of PSCs. The higher working temperature breaks the bonds between molecules and improves carrier recombination. The unnecessary loss of charge carriers by recombination limits the actual potential of the solar cells. As seen from Eq. (3), the higher temperature significantly influences the J-V curve (**Figure 20**). Although degradation and recombination occurred at higher operating temperatures, sometimes a slightly higher temperature than the room temperature can increase the performance of the device by increasing the thermal concentrations [65].

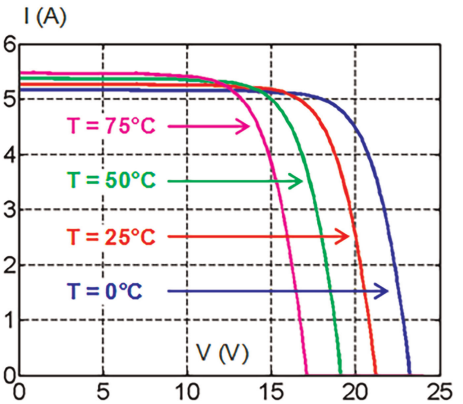


Figure 20.
Impact of working temperature on J-V curve. (Source: https://www.dekloo.net/projets/photovoltaique-autoconsommation/caracteristiques-panneau-photovoltaique/689).

However, the thermal stability can be significantly improved by the morphological variant of perovskite crystals. The morphology of large-scale perovskite crystals will not decompose easily in higher working temperatures as the rate of thermal decomposition, an endothermic and exothermic reaction is completely suppressed by the large morphology of crystals and reduces the self-heating property of perovskites [24]. In large-scale crystals, longer and more stable bonds between the molecules are formed, which facilely decompose under the higher operating temperature and reduce the rate of decomposition [58]. The long-range morphology like micro-rods is formed by stacking of crystallographic planes; hence, heat may not penetrate and break the compact arrangement of crystal planes which efficiently increases the self-life and thermal stability of the perovskites and reduces the degradation [66]. This strategy of tuning the size and scale of perovskites can also improve the thermal stability of the device.

3. All-inorganic metal halide ($CsMX_3$) perovskite solar cells

Nowadays, all-inorganic metal halide perovskite ($CsMX_3$, where M = Cs, Sn, X = Cl, Br, I) semiconductors have drawn increased attention in the development of PSCs, because of superior thermal, electronic, and photovoltaic properties [67–70]. Several studies revealed that 10–11% of all-inorganic lead halide PSCs performed as indicated [71]. However, more groundbreaking research and efforts are needed to raise the power conversion efficiency (PCE) to 25% [34]. The excellent intrinsic stability toward moisture is obtained by the cesium-based perovskite materials with an average efficiency of 10.26% [71]. The PCE of $CsMX_3$-based PSCs has sharply grown from 2.9 to 17.1% with much-improved stability since it was first published in 2015 [72]. The $CsMX_3$ has several morphologies including single-crystal and polycrystalline bulk films. $CsMX_3$ perovskite crystals can be prepared by solution-processed and bottom-up growth methods. $CsMX_3$-based perovskite shows excellent mobility and high PLQY; based on this property, $CsMX_3$ has been developed to apply to solar cells, photodetectors, and LEDs [73, 74].

In all-inorganic perovskites, $CsPbI_3$ is the best candidate for photovoltaic application with a cubic α phase and the narrowest bandgap of 1.73 eV can absorb a wide

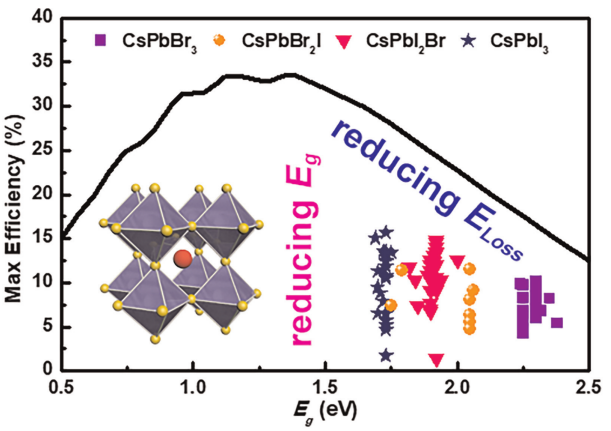


Figure 21.
The PCE of $CsMX_3$-based PSCs has abruptly increased to 17.1% [72].

range of solar radiation. When the bromide anion takes the place of the halide anion, the bandgap increases to 2.3 eV. The mixed-anion $CsPbI_2Br$ and $CsPbIBr_2$ exhibit a bandgap of 1.92 and 2.05 eV (**Figure 21**) [75]. $CsPbBr_2Cl$ is a new class of all-inorganic lead halide perovskite that needs to be explored. The polycrystalline nature of $CsPbBr_2Cl$ with a bandgap of 2.57 eV may be beneficial for the upcoming perovskite-based device. The $CsPbBr_2Cl$ has not been employed yet as a PSC due to the large bandgap [76]. However, these wide-bandgap perovskites have great potential in the field of multi-junction solar cells, LEDs, and photodetectors in combination with the low-bandgap perovskites [72].

4. Emerging Pb-free halide perovskite solar cells

The halide perovskites contain lead, which is a heavy metal that produces a toxic organic and inorganic compound that is hazardous to the environment. Therefore, it is important to investigate Pb-free light-absorbing metal halide materials, with elements such as tin (Sn), germanium (Ge), bismuth (Bi), and antimony (Sb), which can replace the Pb. For this reason, $CsSnX_3$, a Sn-based material free of Pb, can be an excellent alternative [77]. The oxidation of Sn^{2+} ions into Sn^{4+} ions, which is more stable than Sn^{2+} ions, causes Pb-free Sn-based perovskites $CsSnX_3$ to still have stability problems, but it also makes them extremely vulnerable to oxygen and moisture in the air [78].

Numerous studies on the synthesis process and solar applications of $CsSnX_3$-based perovskites have been published recently. The Cs_2SnX_6-based perovskite crystal phase was synthesized by Kaltzoglou et al. [79], who also reported a photovoltaic performance of 4.23% (**Table 1**). The PCE of Sn-based PSCs is still less than that of lead halide PSCs even if they do not have inherent toxicity. A Cs2SnI6-based perovskite structure with a bandgap of 1.48 eV and 1% efficiency was reported by Qiu et al. [81]. ZnO was used as the ETL, and Xiaofeng et al. [80] reported Cs2SnI6 PSC with an efficiency of 0.857%. They made use of HTL-P3HT and ETL-ZnO, the two inorganic absorber layers. $Cs_2SnCl_{6-x}Br$ photodetectors were reported by Jun et al. [87], while Cs_2SnCl_6 perovskite crystals were examined by Hongdan et al. [88]. According to Pujiarti et al. [82], the PCE of the FTO/TiO_2/Cs_2SnI_6/Au PSC combination was 3.94%.

Currently, limited research work has been reported on Cs_2SnI_6-based perovskites, as this class of perovskite is still in the developing stage and a lot of investigation on

Device configuration	Voc (V)	Jsc (mA/cm^2)	FF (%)	PCE (%)
FTO/ZnO/Cs_2SnI_6/P3HT/Au [80]	0.52	3.20	51.50	0.857
FTO/TiO_2/Cs_2SnI_6/HTL/Ag [81]	0.51	5.41	32.0	1.0
FTO/TiO_2/Cs_2SnI_6/N719Dye/Pt [82]	0.67	16.3	61.8	6.8
FTO/TiO_2/Cs_2SnI_6/P3HT/Ag [83]	0.256	7.41	24	0.47
FTO/CdS/Cs_2SnI_6/C/Ag [84]	0.86	0.33	37	0.11
ITO/B-c-$CsSnI_3$/Cs_2SnI_6/Au [85]	0.63	6.1	28	1.1
FTO/PCBM/$CsGe_{0.5}Sn_{0.5}I_3$/Native oxide/Spiro-OMeTAD/Au [86]	18.41	0.63	61.3	7.11

Table 1.
Device performance comparison of PCE of Cs_2SnI_6-based PSCs.

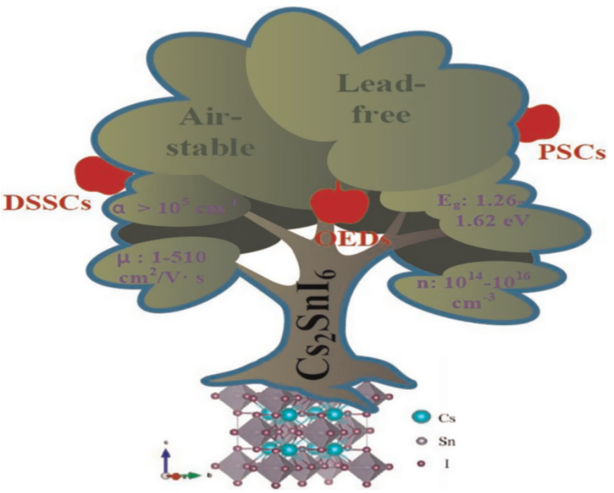


Figure 22.
Air stable and lead-free Cs_2SnI_6 is the next big thing in photovoltaics [89].

the structural, optical, and morphological is required to fully explore and understand the optoelectronic nature of the Cs_2SnI_6. The non-toxic nature and efficiency already accomplished in Cs_2SnI_6-based perovskite are not completed and fulfilled by this class of compounds. The various photovoltaic properties like bandgap and carrier mobility of Cs_2SnI_6-based perovskite material are shown in (**Figure 22**). The Cs_2SnI_6-based perovskite can be used in PSCs, LEDs, and dye-sensitized solar cells (DSSCs). The reported PCE by the Cs_2SnI_6-based PSCs is very low as compared to other classes of perovskites, hence various plenty rooms for these materials need to be filled by intense and seminal scientific and research work like compositional engineering, bandgap tuning, and synthesis methods to fascinating the highest efficiency and environmentally stable PSCs to fill the electricity requirements.

5. Challenges in the synthesis and commercialization of perovskite solar cells

Although PSCs have achieved rapid development in the field of photovoltaic technology in recent years, despite the PCE of PSCs touching the limit of Si-technology, the critical challenges in the synthesis process still limit their commercialization. However, to touch the S-Q limit, the efficiency of PSCs still needs to be improved. The fabrication process of PSCs mainly relied on a well-controlled environment, which is generally an inert gas (N_2)-filled glovebox. Inside a glovebox, a very small area of fabrication of PSCs is possible, which impedes its large area roll-to-roll ambient air scalable fabrications process. On the other hand, the fabrication of ETL, HTL, and perovskite layers under ambient conditions greatly affected the morphology, rate of nucleation, crystallization, and growth.

The poor voids/pinholes, non-uniform, and uneven spread on the surface of the glass substrate become a major challenge in the fabrication process. It is well believed that a good quality perovskite layer is responsible for the excellent photovoltaic performance of PSCs, which strongly rely on the formation dynamic of perovskite

films. The synthesis process of the perovskite layer on the substrate also depends on the interaction between the perovskite precursor solution and the substrate. The perovskite layer faces several degradations and oxidation issues during the synthesis process in ambient air due to oxygen and moisture. The attack of oxygen molecules on perovskite decomposes into constituent perovskite molecules, which hindered the thermal stability of perovskites.

The doctor blade deposition and successive ionic layer adsorption and reaction (SILAR) method are one of the simplest large-scale and cost-effective film deposition techniques that have been widely used to fabricate perovskite thin film with uniformity and high crystallinity [90, 91]. It is also reported that the root mean square (RMS) of the roughness in the doctor-bladed (1.05 nm) and spin-coated (0.98 nm) $CsPbBr_3$ thin films are substantially equivalent [53]. However, the synthesis process by the doctor blade method is also attacked by oxygen and moisture leading to unsmooth perovskite film. The impurity doping, additive in the precursor solution, and compositional engineering may fill the voids/pinholes and provide smoother, compact, and uniform perovskite film [73].

In addition to this important area role in the fabrication of the perovskite layer, a certain amount of additive, such as nanoparticles with perovskite base material, is reported to improve the morphology, optical, and electrical properties of the perovskite light-harvesting layer, thereby improving the photovoltaic performances of PSCs [70, 92–97]. Nevertheless, organic additive materials like polyethylene oxide (PEO)-based precursor solution showed a high photoluminescence quantum yield (PLQY) of 60% when placed as a thin layer of perovskite $CsPbX_3$ [98]. Perovskite thin films are destroyed because PEO, an organic polymer material, is rapidly destroyed by moisture and necessitates intricate processing [99]. We require a stable additive that is resistant to environmental oxygen and moisture to enhance the quality of thin films. ZnO nanoparticles (NPs) support perovskite $CsPbX_3$ thin film for the photovoltaic performance of PSCs because ZnO is an inorganic and thermally stable material [73, 99]. In comparison to a pristine perovskite film, the NP-assisted films had fewer voids and a lower RMS roughness. The $CsPbBr_2Cl$ perovskite layer was stabilized by the solvent vapor treatment, which also increased crystallization and provided density [100–102]. To achieve homogeneous and dense perovskite films in PSCs, however, several other factors must also be taken into account throughout the production process, including processing temperature, environment, and crystallization rate [103]. This method of raising the perovskite film's quality considerably enhances its optical and morphological characteristics, which raises the device's PCE because efficiency depends on the morphology of the film.

6. Conclusion

This chapter emphasizes the need for global energy demand as well as the energy supplies that are currently available. In order to obtain the most effective photovoltaic device, this article systematically explains the perovskite energy harvesting semiconductor with intriguing photovoltaic properties. This article introduces the impact of photovoltaic parameters on the stability and performance of the device, including the thickness, bandgap, electron affinity, mobility, dielectric permittivity, density of states, donor and acceptor density, and defect level of different functional layers of photovoltaic device. The chapter will also address the difficulties surrounding the toxicity of lead and its potential substitution with environmentally friendly, non-toxic

perovskite. This chapter further emphasizes understanding the theoretical mechanisms for modifying the device's photovoltaic features and modeling components that have different stoichiometry to optimally utilize its solar energy production.

Conflict of interest

There is no conflict of interest.

Author details

Asha Chauhan[1*], Anjali Oudhia[2] and Ashok Kumar Shrivastav[1]

1 Department of Physics, National Institute of Technology Raipur, Chhattisgarh, India

2 Department of Physics, Government Nagarjuna Science P.G. College Raipur, Chhattisgarh, India

*Address all correspondence to: ashachauhan.phy@gmail.com

IntechOpen

© 2024 The Author(s). Licensee IntechOpen. This chapter is distributed under the terms of the Creative Commons Attribution License (http://creativecommons.org/licenses/by/4.0), which permits unrestricted use, distribution, and reproduction in any medium, provided the original work is properly cited. CC BY

References

[1] Smil V. Global Solar Energy Consumption, Measured in Terawatt-Hours, Energy Transitions: Global and National Perspectives. BP Statistical Review of World Energy [Internet]. University of Oxford; 2017. Available from: https://ourworldindata.org/grapher/global-primary-energy?country=~OWID_WRL

[2] Polman A, Knight M, Garnett EC, Ehrier B, Sinke WC. Photovoltaic materials: Present efficiencies and future challenges. Science. 2016;**15**(352):6283. DOI: 10.1126/science.aad442

[3] Goldschmidt VM. Die Gesetze der Krystallochemie. Die Naturwissenschaften. 1926;**14**:477-485. DOI: 10.1007/BF01507527

[4] Cristina A. Crystal chemistry, stability and properties of interlanthanide perovskites: A review. Journal of the European Ceramic Society. 2017;**37**(2):427-440. DOI: 10.1016/j.jeurceramsoc.2016.08.041

[5] Jena AK, Kulkarni A, Miyasaka T. Halide perovskite photovoltaics: Background, status and future prospects, chemical reviews. ACS Chemical Reviews. 2019;**13**(119):3036-3103. DOI: 10.1021/acs.chemrev.8b00539

[6] Cao J, Yan F. Recent progress in tin-based perovskite solar cells. Energy & Environmental Science. 2021;**14**:1286. DOI: 10.1016/j.mtener.2021.100891

[7] Yi Z, Ladi NH, Shai X, Li H, Shen Y, Wang M. Will organic-inorganic hybrid halide lead perovskites to be eliminated from optoelectronic applications? Nanoscale Advances. 2019;**1**:1276-1289. DOI: 10.1039/C8NA00416A

[8] Assirey EAR. Perovskite synthesis, properties, and their related biochemical and industrial application. Saudi Pharmaceutical Journal. 2019;**27**:817-829. DOI: 10.1016/j.jsps.2019.05.003

[9] Zhu Y, Deng K, Sun H, Gu B, Lu H, Cao F, et al. TiO_2 phase junction electron transport layer boosts the efficiency of planar perovskite solar cells. Advanced Science. 2018;**5**(1):1700471. DOI: 10.1002/advs.201700614

[10] Li Z, Yang M, Park JS, Wei SH, Berry JJ, Zhu K. Stabilizing perovskite structures by tunning tolerance factor: Formation of formamidinium and cesium lead iodide solid-states alloys. Chemistry of Materials. 2016;**28**(1):284-292. DOI: 10.1021/acs.chemmater.5b04107

[11] Choudhury BD, Ibarra B, Cesano F, Mao Y, Huda MN, Chowdhury AR, et al. The photon absorber and interconnecting layers in multijunction organic solar cells. Solar Energy. 2020;**201**:28-44. DOI: 10.1016/j.solener.2020.02.035

[12] Jiang Y, Yuan J, Ni Y, Yang J, Wang Y, Jiu T, et al. Reduced-dimensional α-$CsPbX_3$ perovskites for efficient and stable photovoltaics. Joule. 2018;**2**(7):1356-1368. DOI: 10.1016/j.joule.2018.05.004

[13] Ghosh D, Ali MY, Chaudhary DK, Bhattacharyya S. Dependence of halide composition on the stability of highly efficient all-inorganic cesium lead halide perovskite quantum dot solar cells. Solar Energy Materials and Solar Cells. 2018;**185**:28-35. DOI: 10.1016/j.solmat.2018.05.002

[14] Ou Q, Bao X, Zhang Y, Shao H, Xing G, Li X, et al. Band structure

engineering in metal halide perovskite nanostructures for optoelectronic applications. Nano Materials Science. 2019;**1**:268-287. DOI: 10.1016/j.nanoms.2019.10.004

[15] Sutherland BR, Sargent EH. Perovskite photonic sources. Nature Photon. 2016;**10**:295-302. DOI: 10.1038/nphoton.2016.62

[16] Lin Q, Armin A, Nagiri RCR, Burn PL, Meredith P. Electro-optics of perovskite solar cells. Nature Photonics. 2014;**9**:106-112. DOI: 10.1038/nphoton.2014.284

[17] Dong Q, Fang Y, Shao Y, Mulligan P, Qiu J, Cao L, et al. Electron-hole diffusion lengths > 175 μm in solution-grown $CH_3NH_3PbI_3$ single crystals. Science. 2015;**347**:967-970. DOI: 10.1126/science.aaa5760

[18] Frolova LA, Dremova NN, Troshin PA. The chemical origin of the p-type and n-type doping effects in the hybrid methylammonium-lead iodide ($MAPbI_3$) perovskite solar cells. Chemical Communications. 2015;**51**:14917-14920. DOI: 10.1039/C5CC05205J

[19] Shi D, Adinolfi V, Comin R, Yuan M, Alarousu E, Buin A, et al. Solar cells low trap-state density and long carrier diffusion in organolead trihalide perovskite single crystals. Science. 2015;**347**:519-522. DOI: 10.1126/science.aaa2725

[20] Motta C, Mellouhi FE, Sanvito S. Charge carrier mobility in hybrid halide perovskites. Scientific Reports. 2015;**5**:12746. DOI: 10.48550/arXiv.1411.7904

[21] Fan GY, Jing DH, Nan LN, Lei Y, Yu ZC. Effect of carrier mobility on the performance of perovskite solar cells. Chinese Physics B. 2019;**28**(4):048802

[22] Baranowski M, Plochocka P. Excitons in metal-halide perovskites. Advanced Energy Materials. 2020;**10**(26):1903659. DOI: 10.1002/aenm.201903659

[23] Haeger T, Heiderhoff R, Riedl T. Thermal properties of metal-halide perovskites. Journal of Materials Chemistry C. 2020;**8**:14289-14311. DOI: 10.1039/D0TC03754K

[24] Mishra A, Ahmad Z, Touati F, Shakoor RA, Nazeeruddin MK. One-dimensional facile growth of $MAPbI_3$ perovskite micro-rods. RSC Advances. 2019;**9**:11589-11594. DOI: 10.1039/C9RA00200F

[25] NREL Efficiency chart. Available from: https://www.nrel.gov/pv/assets/pdfs/best-research-cell-efficiencies.20190802.pdf

[26] Meng L, You J, Yang Y. Addressing the stability issue of perovskite solar cells for commercial applications. Nature Communications. 2018;**9**:5265. DOI: 10.1038/s41467-018-07255-1

[27] Manser JS, Christians JA, Kamat PV. Intriguing optoelectronic properties of metal halide perovskites. Chemical Reviews. 2016;**116**(21):12956-13008. DOI: 10.1021/acs.chemrev.6b00136

[28] Sum TC, Mathews N. Advancements in perovskite solar cell: Photophysics behind the photovoltaics. Advanced Science. 2018;**5**(3):1700614. DOI: 10.1039/C4EE00673A

[29] Liang X, Ge C, Fang Q, Deng W, Dey S, Lin H, et al. Flexible perovskite solar cells: Progress and prospects. Frontiers in Materials. 2021;**8**:634353. DOI: 10.3389/fmats.2021.634353

[30] Borowski M. Perovskites: Structure, Properties and Uses (Chemical

Engineering Methods and Technology). UK ed. Nova Science Publishers, Inc; 30 Mar 2011. ISBN: 978-1-61668-525-6

[31] Andrea C, Ole H. What are the band alignments of $Cu_2ZnSn(S, Se)_4$ solar cells? Solar Energy Materials and Solar Cells. 2017;**169**:177-194. DOI: 10.1016/j.solmat.2017.05.008

[32] Sarunas S, Sergejus B, Mantas S, Gediminas U, Martynas K, Martynas V, et al. Phase transitions, screening, and dielectric response of $CsPbBr_3$. Journal of Materials Chemistry A. 2020;**8**: 14015-14022. DOI: 10.1039/D0TA04155F

[33] Chauhan A, Oudhia A, Shrivastav AK, Tirkey OS. Performance enhancement of an all-inorganic perovskite solar cell by using SCAPS and DFT extracted parameters of CuX (X = I, Cl, Br). Material Chemistry and Physics. 2023;**309**:128327. DOI: 10.1016/j.matchemphys.2023.128327

[34] Yassine R, Hamid EZ, Samrana K, Shahzada A. Energy level engineering of charge selective contact and halide perovskite by modulating band offset: Mechanic insights. Journal of Energy Chemistry. 2021;**54**:822-829. DOI: 10.1016/j.jechem.2020.06.030

[35] Guoqing T, Taotao C, Huan L, Wentao S, Yajing C, Jingling L, et al. Highly efficient hole extraction and stable all-bromine inorganic perovskite solar cells via derivative-phase gradient bandgap. Advanced Science News Solar RRL. 2019;**3**(5):1900030. DOI: 10.1002/solr.201900030

[36] Liu N, Chen MM, Yang H, Yang H, Ran M, Zhang C, et al. TiO_2/Mg-SnO_2 nanoparticle composite compact layer for enhancing the performance of perovskite solar cells. Optical Materials Express. 2020;**10**(1):157-169. DOI: 10.1364/OME.380354

[37] Mahmood K, Sarwar S, Mehran MT. Current status of electron transport layers in perovskite solar cells: Materials and properties. RSC Advances. 2017;**7**: 17044. DOI: 10.1039/C7RA00002B

[38] Yasin S, Zoubi TA, Moustafa M. Design and simulation of high-efficiency lead-free heterostructure perovskite solar cell using SCAPS-1D. Optik. 2021; **229**:166258. DOI: 10.1016/j.ijleo.2021.166258

[39] Bag A, Radhakrishnan R, Nekovei R, Jeyakumar R. Effect of the absorber layer, hole transport thickness and its doping density on the performance of perovskite solar cells by device simulation. Solar Energy. 2020;**196**: 177-182. DOI: 10.1016/j.solener.2019.12.014

[40] Ullah S, Liu P, Wang J, Yang P, Liu L, Yang SE, et al. Optimizing the working mechanism of the $CsPbBr_3$-based inorganic perovskite solar cells for enhanced efficiency. Solar Energy. 2020; **209**:79-84. DOI: 10.1016/j.solener.2019.12.014

[41] Chauhan A, Oudhia A. First-principle density functional theory-derived nonleaded $KSn_{1-x}Ge_xI_3$-based perovskite solar cells: A theoretical study. Energy Technology. 2023;**12**(2): 2300772. DOI: 10.1002/ente.202300772

[42] Lee YM, Maeng I, Park J, Song M, Yun JH, Jung MC, et al. Comprehensive understanding and controlling the defect structure: An effective approach for organic-inorganic hybrid perovskite-based solar-cell application. Journal of Solid State Chemistry. 2018;**205**:39-43. DOI: 10.3389/fenrg.2018.00128

[43] Ball JM, Petrozza A. Defects in perovskite-halides and their effects in solar cells. Nature Energy. 2016;**1**:16149. DOI: 10.1038/nenergy.2016.149

[44] Abdelaziz S, Zekry A, Shaker A, Abouelatta M. Investigating the performance of formamidinium tin-based perovskite solar cell by SCAPS device simulation. Optical Materials. 2020;**101**:109738. DOI: 10.1016/j.optmat.2020.109738

[45] Patel PK. Device simulation of highly efficient eco-friendly $CH_3NH_3SnI_3$ perovskite solar cell. Scientific Reports. 2021;**11**:3082. DOI: 10.1038/s41598-021-82817-w

[46] Chauhan A, Shrivastav AK, Oudhia A. Synthesis and characterization of ambient processed FTO/ZnO/$CsPbBr_2Cl$/C perovskite solar cell deposited by SILAR method. Optical Materials. 2022;**130**:112575. DOI: 10.1016/j.optmat.2022.112575

[47] Pratheek M, Abhinav T, Bhattacharya S, Chandra GK, Predeep P. Recent progress on defect passivation in perovskites for a solar cell application. Materials Science for Energy Technologies. 2021;**4**:282-289. DOI: 10.1016/j.mset.2021.07.003

[48] Lin CT, Rossi FD, Kim J, Baker J, Ngiam J, Xu B, et al. Evidence for surface defect passivation as the origin of the remarkable photostability of unencapsulated perovskite solar cells employing aminovaleric acid as a processing additive. Journal of Materials Chemistry A. 2019;**7**:3006-3011. DOI: 10.1039/C8TA11985F

[49] Akbulatov AF, Frolova L, Tsarev SA, Zhidkov IS, Luchkin S, Kurmaev EZ, et al. Film deposition techniques impact defect density and photostability of $MAPbI_3$ perovskite films. Journal of Physical Chemistry C. 2020;**124**(39):21378-21385. DOI: 10.1021/acs.jpcc.0c07673

[50] Tavakoli MM, Gu L, Gao Y, Reckmeier C, He J, Rogach AL, et al. Fabrication of efficient planar perovskite solar cells using a one-step chemical vapor deposition method. Scientific Reports. 2015;**5**:14083. DOI: 10.1038/srep14083

[51] Chen CW, Kang HW, Hsiao SY, Yang PF, Chiang KM, Lin HW. Efficient and uniform planar-type perovskite solar cells by simple sequential vacuum deposition. Advanced Materials. 2014; **26**(38):6647-6652. DOI: 10.1002/adma.201402461

[52] Leyden MR, Ono LK, Raga SR, Kato Y, Wang S, Qi Y. High-performance perovskite solar cells by hybrid chemical vapor deposition. Journal of Materials Chemistry. 2014; **2**:18742-18745. DOI: 10.1039/C4TA04385E

[53] Noor BM, Ahmed FH, Ammar EAK. Study of mechanical properties of Wollastonite filled epoxy functionally graded composite. International Journal of Mechanical Engineering and Technology. 2018;**9**:669-677

[54] Wang F, Bai S, Tress W, Hagfeldt A, Gao F. Defects engineering for high-performance perovskite solar cells. npj Flexible Electronics. 2018;**2**:22. DOI: 10.1038/s41528-018-0035-z

[55] Yang WS, Noh JH, Jeon NJ, Kim YC, Ryu S, Seo J, et al. High-performance photovoltaic perovskite layers fabricated through intramolecular exchange. Science. 2015; **348**(6240):1234-1237. DOI: 10.1126/science.aaa9272

[56] Tailor NK, Satapathi S. The impact of $Cs_3Bi_2Cl_9$ single crystal growth modality on its symmetry and morphology. Journal of Materials Research and Technology. 2020;**9**(4): 7149-7157. DOI: 10.1016/j.jmrt.2020.04.097

[57] Gillespie C. How Does Temp Affect the Growth Rate of Crystals? Available from: https://sciencing.com/temp-affect-growth-rate-crystals-6318908.html 26 April 2018

[58] Niu G, Li W, Wang J. Progress of interface engineering in perovskite solar cells. Science China Materials. 2016;**59**: 728-742. DOI: 10.1007/s40843-016-5094-6

[59] Chen S, Liu X, Wang Z, Li W, Gu X, Lin J, et al. Defect passivation of $CsPbBr_3$ with AgBr for high-performance all-inorganic perovskite solar cells. Advanced Energy and Sustainability Research. 2016;**2**(6):2000099. DOI: 10.1002/aesr.202000099

[60] Semwal BS, Panwar NS. Dielectric properties of perovskite crystals. Bulletin of Materials Science. 1992;**15**:237. DOI: 10.1002/9781118935651.ch6

[61] Yang D, Yang R, Wang K, Wu C, Zhu X, Feng J, et al. High-efficiency planar-type perovskite solar cells with negligible hysteresis using EDTA-completed SnO_2. Nature Communications. 2018;**9**:3239. DOI: 10.1038/s41467-018-05760-x

[62] Mehrabian M, Afshar EN, Yousefzadeh SA. Simulating the thickness effect of the graphene oxide layer in $CsPbBr_3$-based solar cells. Materials Research Express. 2021;**8**: 35509. DOI: 10.1088/2053-1591/abf080

[63] Raj A, Kumar M, Bherwani H, Gupta A, Anshul A. Evidence of improved power conversion efficiency in lead-free $CsGeI_3$-based perovskite solar cell heterostructure via scaps simulation. Journal of Vacuum Science and Technology B. 2021;**39**:012401. DOI: 10.1116/6.0000718

[64] Mesquita I, Andrade L, Mendes A. Temperature impact on perovskite solar cells under operation. ChemSusChem. 2019;**12**(10):2186-2194. DOI: 10.1002/cssc.201802899

[65] Yadav P, Tripathi B, Lokhande M, Kumar M. Effect of temperature and concentration on commercial silicon module-based low-concentration photovoltaic system. Journal of Renewable and Sustainable Energy. 2013;**5**:013113. DOI: 10.1063/1.4790817

[66] Ding GQ, Shen WZ, Zheng MJ, Fan DH. Synthesis of ordered large-scale ZnO nanopore arrays. Applied Physics Letters. 2006;**88**(10):103106. DOI: 10.1063/1.2182025

[67] Son DY, Im JH, Kim HS, Park NG. 11% efficient perovskite solar cell based on ZnO nanorods: An effective charge collection system. The Journal of Physical Chemistry C. 2014;**118**(30): 16567-16573. DOI: 10.1021/jp412407j

[68] Zonglong Z, Yang B, Xiao L, Chu CC, Shihe Y, Alex K, et al. Enhanced efficiency and stability of inverted perovskite solar cells using highly crystalline SnO_2 nanocrystals as the robust electron-transporting layer. Advanced Materials. 2016;**28**(30): 6478-6484. DOI: 10.1002/adma.201600619

[69] Jie L, Fei G, Haoxu W, Juan L, Jiexuan J, Xin W, et al. Efficient planar $CsPbBr_3$ perovskite solar cells by dual-source vacuum evaporation. Solar Energy Materials and Solar Cells. 2018; **187**:1-8. DOI: 10.1016/j.solmat.2018.07.009

[70] Yongyi P, Yudiao C, Chunhua W, Chujun Z, Huayan X, Keqing H, et al. Fully doctor-bladed planar heterojunction perovskite solar cells under ambient condition. Organic Electronics. 2018;**58**:153-158. DOI: 10.1016/j.orgel.2018.04.020

[71] Haiwen Y, Yuanyuan Z, Jialong D, Yudi W, Xiya Y, Qunwei T. 10.26%-efficiency all-inorganic $CsPbBr_3$ perovskite solar cell by spectra engineering. Journal of Materials Chemistry A. 2018;**6**:24324. DOI: 10.1039/C8TA08900K

[72] Zhang J, Hodes G, Jin Z, Liu S. All-inorganic $CsPbX_3$ perovskite solar cells: Progress and prospects. Angewandte Chemie International Edition. 2019; **58**(44):15596-15618. DOI: 10.1002/anie.201901081

[73] Cunlong L, Zhigang Z, Ceng H, Zhiping H, Xiaosheng T, Juan D, et al. Enhanced random lasing emission from highly compact $CsPbBr_3$ perovskite thin films decorated by ZnO nanoparticles. Nano Energy. 2017;**40**:195-202. DOI: 10.1016/j.nanoen.2017.08.013

[74] Tongtong X, Xianfeng Y, Sunqi L, Junjian H, Yong L, Jinbo Y, et al. Highly stable $CsPbBr_3$ quantum dots coated with alkyl phosphate for white light-emitting diodes. Nanoscale. 2017;**9**(40): 15286-15290. DOI: 10.1039/C7NR04179A

[75] Deng J, Li J, Yang Z, Wang M. All-inorganic lead halide perovskite: A promising choice for photovoltaics and detectors. Journal of Materials Chemistry. 2019;**5**:1-68. DOI: 10.1039/C9TC04164H

[76] Paul T, Chatterjee BK, Maiti S, Besra N, Thakur S, Sarkar S, et al. Efficient blue emission from ambient processed all-inorganic $CsPbBr_2Cl$ perovskite cubes. AIP Conference Proceedings. 2018;**1942**:120026. DOI: 10.1063/1.5029066

[77] Lee B, Stoumpos CC, Zhou N, Hao F, Malliakas C, Yeh CY, et al. Air-stable molecular semiconducting iodosalts for solar cell applications: Cs_2SnI_6 as a hole conductor. Journal of the American Chemical Society. 2014;**136**(43): 15379-15385. DOI: 10.1021/ja508464w

[78] Xing G, Kumar MH, Chong WK, Liu X, Cai Y, Ding H, et al. Solution-processed tin-based perovskite for near-infrared lasing. Advanced Materials. 2016;**28**:8191-8196. DOI: 10.1002/adma.201601418

[79] Kaltzoglou A, Antoniadou M, Kontos AG, Stoumpos CC, Perganti D, Siranidi E, et al. Optical-vibrational properties of the Cs_2SnX_6 (X = Cl, Br, I) defect perovskites and hole-transport efficiency in dye-sensitized solar cells. Journal of Physical Chemistry C. 2016; **120**:11777-11785. DOI: 10.1021/acs.jpcc.6b02175

[80] Xiaofeng Q, Yanan J, Hailiang Z, Zhiwen Q, Shuai Y, Ping W, et al. Lead-free mesoscopic Cs_2SnI_6 perovskite solar cells using different nanostructured ZnO nanorods as electron transport layers. Physica Status Solidi RRL. 2016; **10**(8):587-591. DOI: 10.1002/pssr.201600166

[81] Qiu X, Cao B, Yuan S, Chen X, Qiu Z, Jiang Y, et al. From unstable $CsSnI_3$ to air-stable Cs_2SnI_6: A lead-free perovskite solar cell light absorber with bandgap of 1.48 eV and high absorption coefficient. Solar Energy Materials and Solar Cells. 2017;**159**:227-234. DOI: 10.1016/j.solmat.2016.09.022

[82] Pujiarti H, Wulandari P, Hidayat R. Photocurrent enhancement by incorporation of air-stable Cs_2SnI_6 perovskite in the dye-sensitized solar cell. Journal of Physics: Conference Series. 2019;**1245**:012066. DOI: 10.1088/1742-6596/1245/1/012066

[83] Jiang Y, Zhang H, Qiu X, Cao B. The air and thermal stabilities of lead-free perovskite variant Cs_2SnI_6 powder.

Materials Letters. 2017;**199**:50-52. DOI: 10.1016/j.matlet.2017.04.046

[84] Suazo FJA, Shaji S, Avellaneda D, Martínez JAA, Krishnan B. Solar cell using spray cast Cs_2SnI_6 perovskite thin films on chemical bath deposited CdS yielding high open-circuit voltage. Journal of Solar Energy. 2020;**207**:486. DOI: 10.1016/j.solener.2020.06.101

[85] Lee B, Krenselewski A, Baik SI, Seidmana DN, Chang RPH. Solution processing of air-stable molecular semiconducting iodosalts, Cs_2SnI_6-XBrX, for potential solar cell applications. Energy & Fuels. 2017;**1**:710. DOI: 10.1039/C7SE00100B

[86] Liu Y, Gao W, Ran C, Dong H, Sun N, Ran X, et al. All-inorganic Sn-based perovskite solar cells: Status, challenges, and perspectives. ChemSusChem. 2020;**13**(24):6477-6497. DOI: 10.1002/cssc.202001680

[87] Jun Z, Jiajun L, Ximing R, Peijia W, Maxim SM, Yang H, et al. Lead-free perovskite derivative $Cs_2SnCl_{6-x}Br_x$ single crystals for narrowband photodetectors. Advanced Optical Materials. 2019;**7**(10):1900139. DOI: 10.1002/adom.201900139

[88] Hongdan Z, Ludan Z, Jun C, Long C, Chuanqi L, Shuanglong Y. Morphologically controlled synthesis of Cs_2SnCl_6 perovskite crystals and their photoluminescence activity. Crystals. 2019;**9**:258. DOI: 10.3390/cryst9050258

[89] Ullah S, Wang J, Yang P, Liu L, Khan J, Yang SE, et al. Lead-free Cs_2SnI_6 perovskites for optoelectronic applications: Recent developments and perspectives. Solar RRL. 2021;**5**(5): 2000830. DOI: 10.1002/solr.202000830

[90] Dehghan M, Behjat A. Deposition of zinc oxide as an electron transport layer in planar perovskite solar cells by spray and SILAR methods comparable with spin coating. RSC Advances. 2019;**9**: 20917-20924. DOI: 10.1039/C9RA01839E

[91] Penga Y, Cheng Y, Wang C, Zhang C, Xia H, Huang K, et al. Fully doctor-bladed planar heterojunction perovskite solar cells under ambient condition. Organic Electronics. 2018;**58**: 153-158. DOI: 10.1016/j.orgel.2018.04.020

[92] Yue P, Haiyan G, Ziyang H, Jing Z, Yuejin Z. $BiBr_3$ as an additive in $CsPbBr_3$ for carbon-based all-inorganic perovskite solar cells. Journal of Alloys and Compounds. 2020;**835**:155283. DOI: 10.1016/j.jallcom.2020.155283

[93] Haonan S, Qingliang L, Zheng Z, Yong L, Xuhui Y, Guangjie Z, et al. An innovative design of perovskite solar cells with Al_2O_3 inserted at the ZnO/perovskite interface for improving performance and stability. Nano Energy. 2016;**22**:223-231. DOI: 10.1016/j.nanoen.2016.02.025

[94] Deng W, Wenjing L, Weihai S, Xuping L, Guodong L, Zibao W, et al. Guanidinium iodide modification enabled highly efficient and stable all-inorganic $CsPbBr_3$ perovskite solar cells. Electrochimica Acta. 2021;**365**:137360. DOI: 10.1016/j.electacta.2020.137360

[95] Yichuan L, Yu T, Xi W, Jamie CW, Javon MK, Fernando PO, et al. Enhanced optical and electrical properties of polymer-assisted all-inorganic perovskite for light emitting diodes. Advanced Materials. 2016;**28**(40): 8983-8989. DOI: 10.1002/adma.201602513

[96] Zhang W, Saliba M, Stranks SD, Sun Y, Wiesner U, Snaith HJ. Enhancement of perovskite-based solar

cells employing core-shell metal nanoparticles. Nano Letters. 2013;**13**(9): 4505-4510. DOI: 10.1021/nl4024287

[97] Liang PW, Liao CY, Chugh CC, Zuo F, Williams ST, Xin XK, et al. Additive enhanced crystallization of solution-processed perovskite for highly efficient planar-heterojunction solar cells. Advanced Materials. 2014;**26**(22): 3748-3754. DOI: 10.1002/adma.2014 00231

[98] Chauntian Z, Liming D. An 80.11% FF record was achieved for perovskite solar cells by using the NH_4Cl additive. Nanoscale. 2014;**6**:9934. DOI: 10.1039/ C4NR02425G

[99] Chauhan A, Shrivastav AK, Oudhia A. Optical, morphological and electrical studies of fully doctor-bladed $CsPbBr_2Cl$-based perovskite thin film. Microelectronic Engineering. 2022;**258**: 111757. DOI: 10.1016/j.mee.2022.111757

[100] Runzhong L, Ke X. Solvent engineering for perovskite solar cells: A review. Micro and Nano Letters. 2020; **15**(6):349-353. DOI: 10.1049/ mnl.2019.0735

[101] Rachma DS, Veinardi S. Isolation of chlorophyll from spinach and its modification using Fe^{2+} in photostability study. In: Proceedings of the Third International Conference on Mathematics and Natural Science; 23'25 November 2010; Bandung, Indonesia. Bandung, Indonesia: Faculty of Mathematics and Natural Sciences, School of Life Sciences and Technology, and School of Pharmacy at Institute Technologist Bandung; 2010. pp. 859-873

[102] Fan Z, Jun S, Ming C, Junchen L, Yuying H, Yuncai W, et al. Enhanced perovskite morphology and crystallinity for high-performance perovskite solar cells using a porous hole transport layer from polystyrene nanospheres. Physical Chemistry Chemical Physics. 2016;**18**: 32903-32909. DOI: 10.1039/ C6CP06405A

[103] Gupta M, Oudhia A, Bisen DP. A review on perovskite solar cell for high-efficiency future applications. International Journal of Luminescence and Applications. 2017;7:413-416